

Gamma ray bursts, Soft gamma repeaters, and Magnetars.

G.S.Bisnovatyi-Kogan

IKI RAS, Moscow and JINR, Dubna

Physics of Neutron Stars, Saint-Petersburg, 25 June, 2008

Estimations

Radiopulsars, GRB, SGR

Naked eye optical afterglow

Magnetars

Nuclear model of SGR

Neutron stars are the result of collapse.

Conservation of the magnetic flux

$$B(\text{ns}) = B(\text{s}) \left(R_s / R_{\text{ns}} \right)^2$$

$$B(\text{s}) = 10 - 100 \text{ Gs}, \quad R_s \sim (3 - 10) R(\text{Sun}), \quad R_{\text{ns}} = 10 \text{ km}$$

$$B(\text{ns}) = 4 \cdot 10^{11} - 5 \cdot 10^{13} \text{ Gs} \quad \text{Ginzburg (1964)}$$

Radiopulsars

$E = AB^2 \Omega^4$ - magnetic dipole radiation (pulsar wind)

$$E = 0.5 I \Omega^2$$

I – moment of inertia of the neutron star

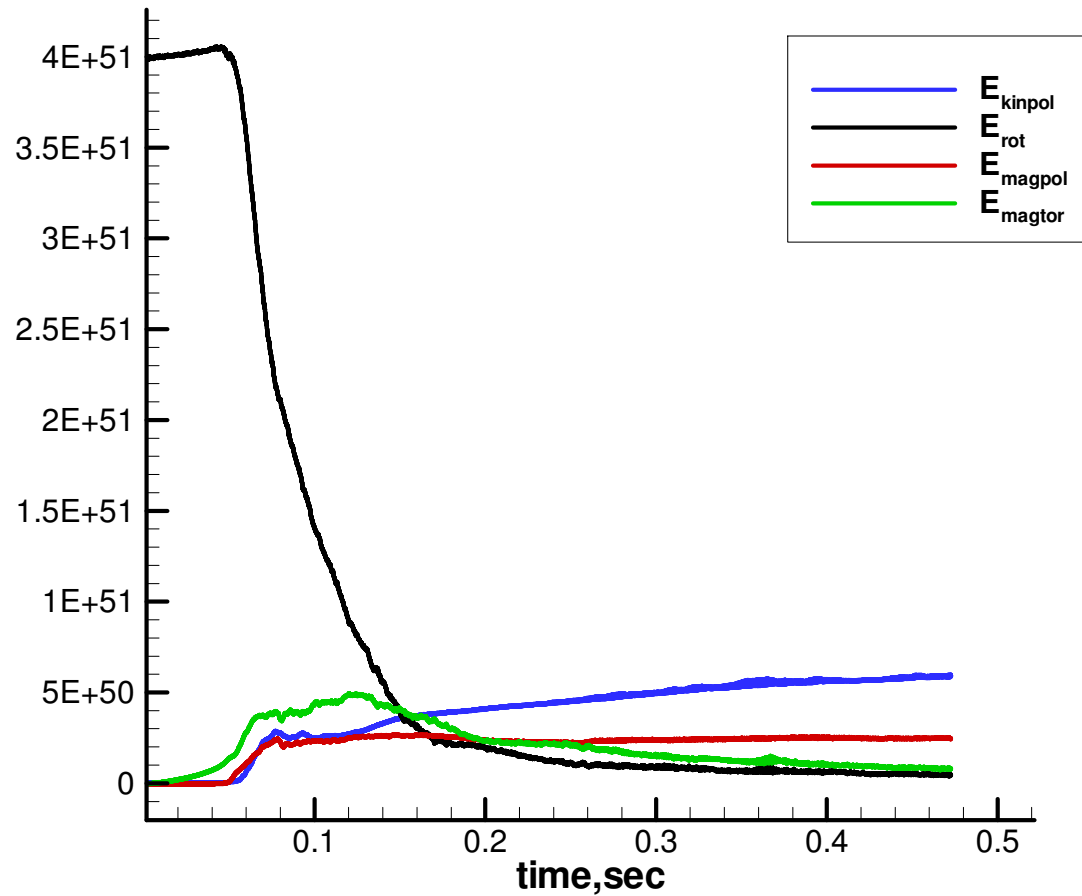
$$B = \frac{I \dot{P}}{4 \pi^2 A}$$

Single radiopulsars – timing observations

(the most rapid ones are connected with young supernovae remnants)

$$B(\text{ns}) = 2 \cdot 10^{11} - 5 \cdot 10^{13} \text{ Gs}$$

Neutron star formation



N.V.Ardeljan,
G.S.Bisnovatyι-Kogan,
S.G.Moiseenko MNRAS,
2005, **359**, 333.

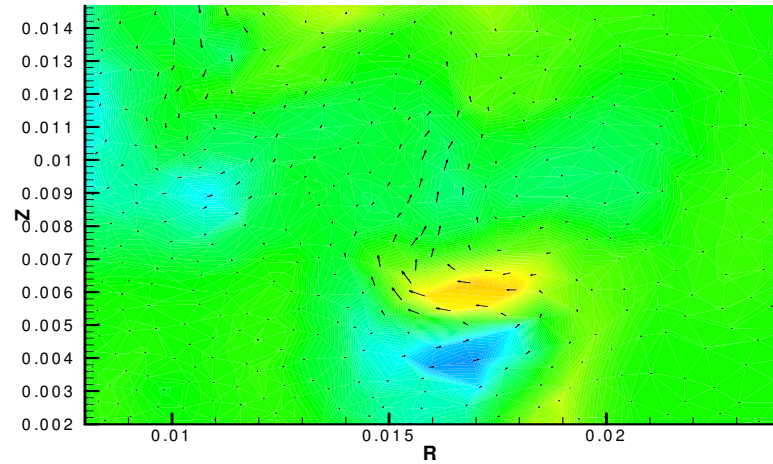
B(chaotic) ~ 10¹⁴ Gs

**High residual chaotic
magnetic field after MRE
core collapse SN explosion.**

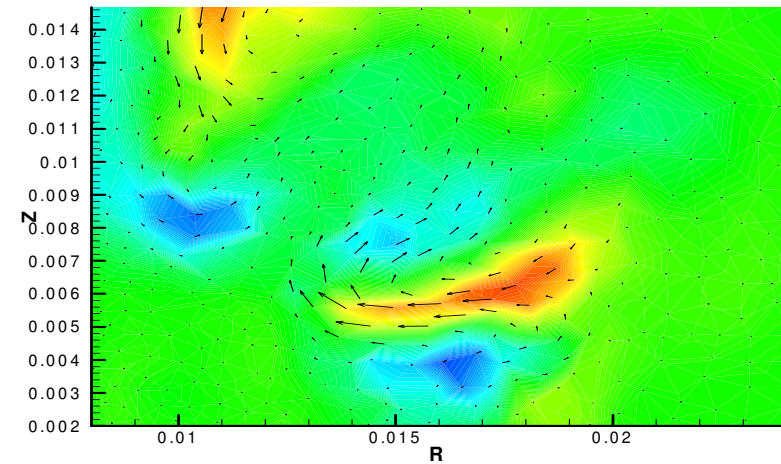
**Heat production during
Ohmic damping of the chaotic
magnetic field may influence
NS cooling light curve**

Inner region: development of magnetorotational instability (MRI)

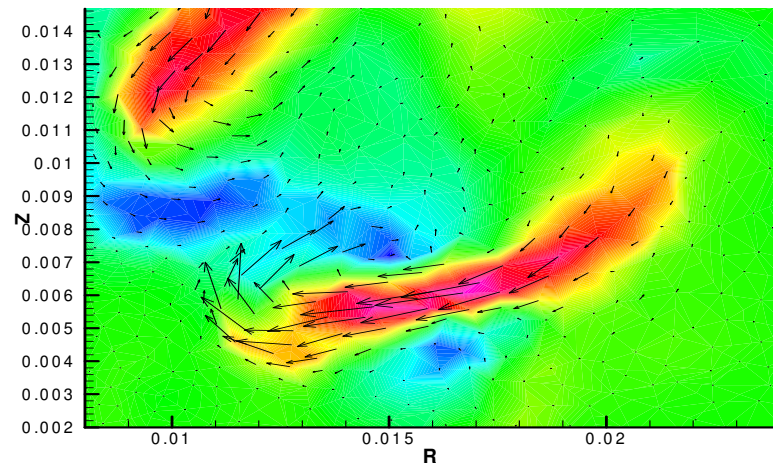
TIME= 34.83616590 (1.20326837sec)



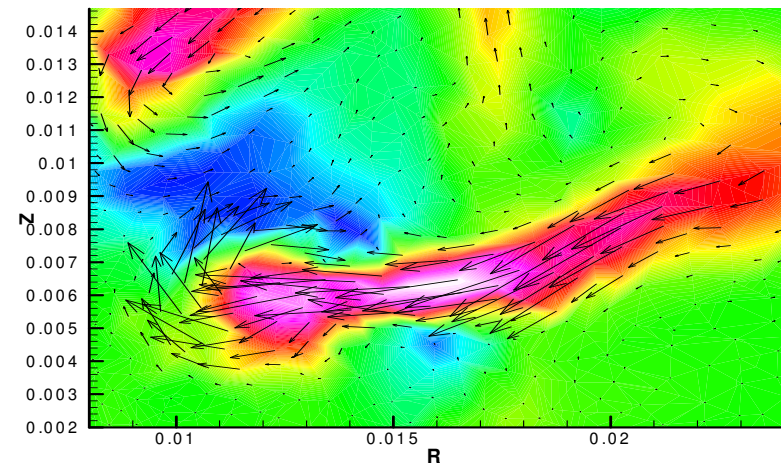
TIME= 35.08302173 (1.21179496sec)



TIME= 35.26651529 (1.21813298sec)



TIME= 35.38772425 (1.22231963sec)



Toy model of the MRI development: exponential growth of the magnetic fields

$$\frac{dH_\varphi}{dt} = H_r \left(r \frac{d\Omega}{dr} \right); \quad \text{at initial stages} \quad H_\varphi < H_\varphi^* : \left(r \frac{d\Omega}{dr} \right) = A \approx \text{const},$$

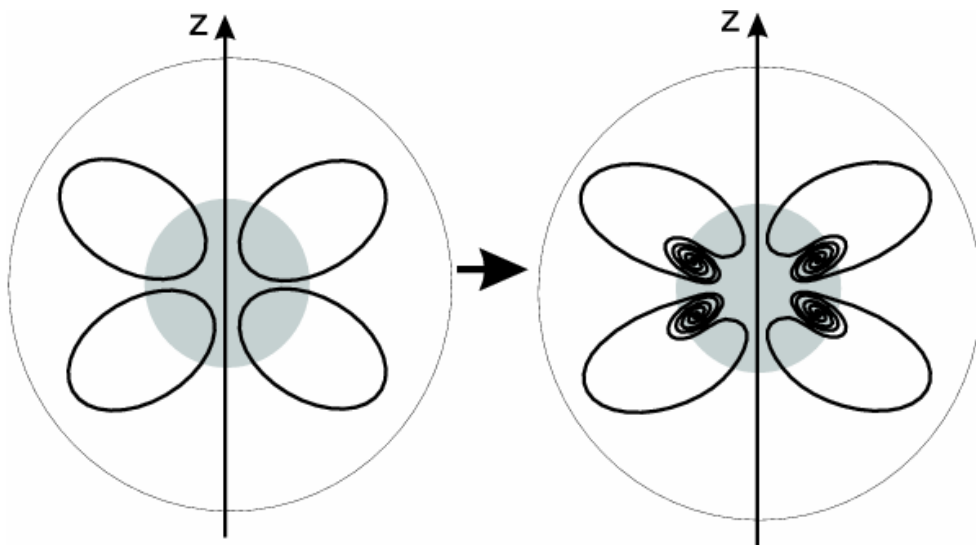
MRI leads to formation of multiple *poloidal* differentially rotating vortices. Angular velocity of vortices is growing (linearly) with a growth of H_φ .

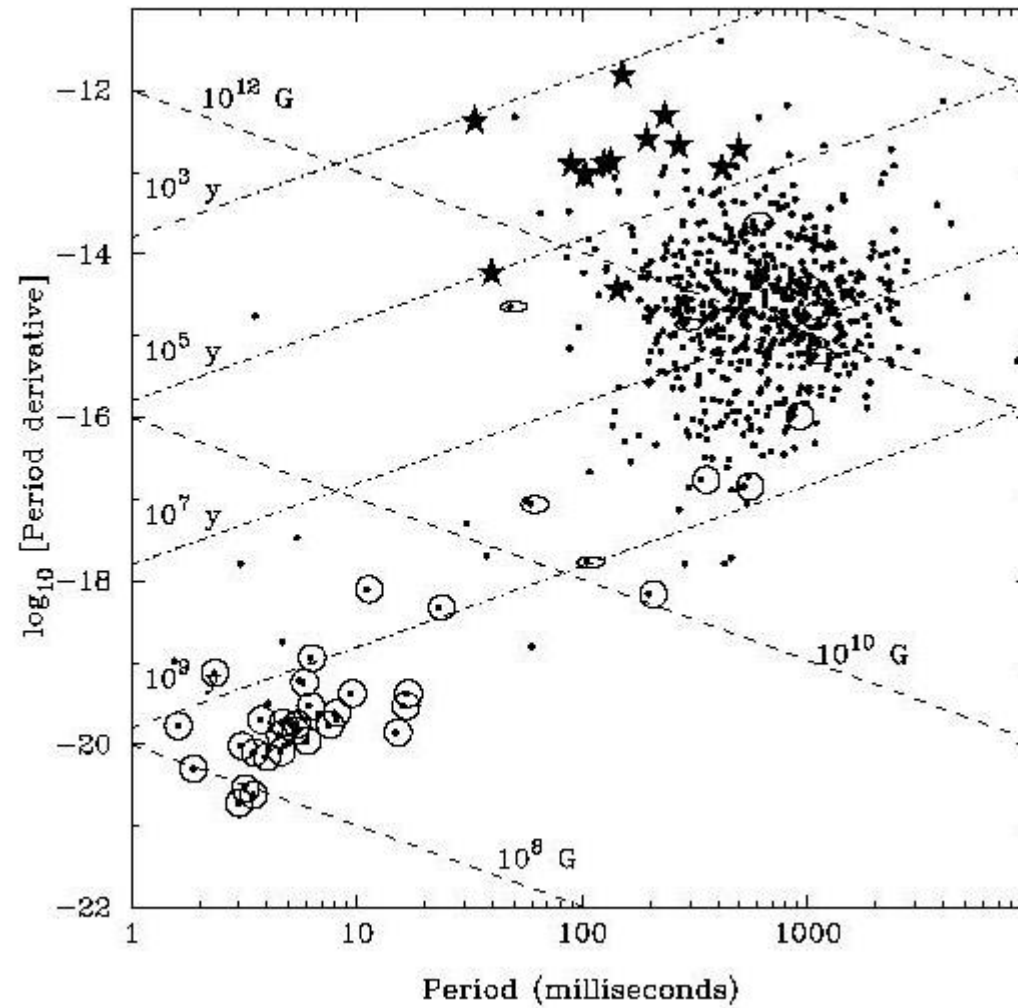
$$\frac{dH_r}{dt} = H_{r0} \left(\frac{d\omega_v}{dl} l \right), \quad \left(\frac{d\omega_v}{dl} l \right) \approx \alpha (H_\varphi - H_\varphi^*).$$

$$\frac{d^2}{dt^2} (H_\varphi - H_\varphi^*) = AH_{r0} \alpha (H_\varphi - H_\varphi^*)$$

⇓

$$\begin{cases} H_\varphi = H_\varphi^* + H_{r0} e^{\sqrt{A\alpha H_{r0}}(t-t^*)}, \\ H_r = H_{r0} + \frac{H_{r0}^{3/2} \alpha^{1/2}}{\sqrt{A}} \left(e^{\sqrt{A\alpha H_{r0}}(t-t^*)} - 1 \right). \end{cases}$$





1973 - GRB discovery (spectrum of nuclear explosion on Earth)

1974 - Prilutski, Usov, first cosmological GRB model: collapse in AGN nuclei

1985 - Berezhinski, Prilutski, GRB from stellar relativistic collapse

$$\nu\bar{\nu} \rightarrow e^+e^- \rightarrow \gamma\gamma$$

$$W_{x,\gamma} \sim 3 \cdot 10^{48} \text{ ergs}, \varepsilon \sim 6 \cdot 10^{-6},$$

$$W_{\nu\bar{\nu}} \sim 6 \cdot 10^{53} \text{ ergs.}$$

Similar models are considered now, about 100.

Observed GRB energy (from redshift z , isotropy)

$$\text{GRB990123: } z \approx 1.6,$$

$$W_\gamma \sim 2.3 \cdot 10^{54} \text{ ergs,}$$

$$W_{opt} \sim 10^{51} \text{ ergs}$$

(around 1 MeV)

GRB from SN

explosion:

Bisnovatyi-Kogan,

Imshennik, Nadyozhin,

Chetkin (1975)

X-rays (Beppo-SAX),

optical telescope, HST

Collimation is needed to decrease the energy

GRB CENTRAL MACHINE MODELS

Hypernova (very powerful supernova).

Paczynski (1998) – explosion of a helium star (see also Blinnikov and Postnov, 1998)

Usov (1992) – new born pulsar, very rapid, with high magnetic field

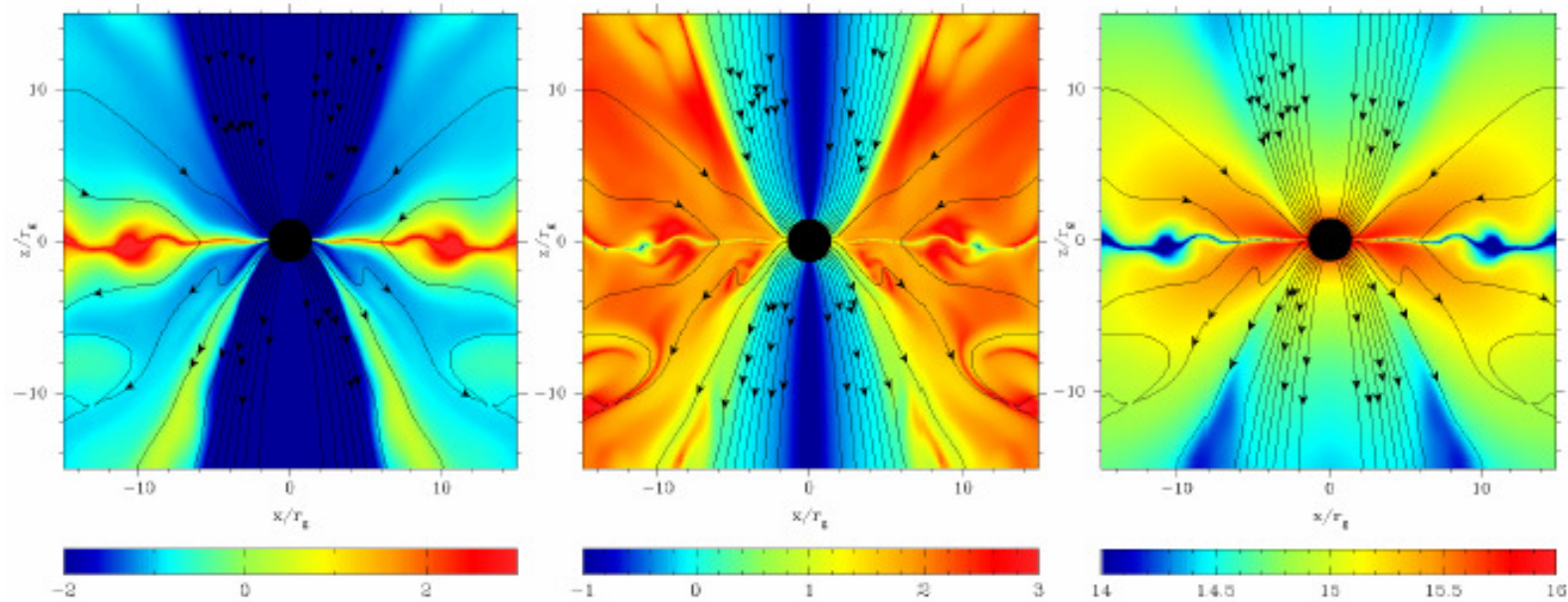
Cherepashchuk, Gershtein et al. (2002) W-R stars as GRB predecessors

Woosley et al. (2001) collapse of very massive star, formation of a black hole with a massive disk

(may be with magnetic field)

Now it is the most popular model. Traces of SNe are believed to be found in optical afterglows of several GRB.

(Barkov, Komissarov, 2007)



The inner region at $t = 0:45s$.

Left panel: the magnetization parameter, $\log_{10}(P/P_m)$, and the magnetic field lines;

Middle panel: the ratio of azimuthal and poloidal magnetic field strengths, $\log_{10}(B_{\phi}/B_p)$, and the magnetic field lines;

Right panel: the magnetic field strength, $\log_{10}(B)$, and the magnetic field lines.

4. Magnetized disk around rotating (Kerr) black hole (RBH)
Van Putten (2001). Extraction of rotational energy of RBH when magnetic field is connecting the RBH with the surrounding accretion disk or accretion torus: Blandford—Znajek mechanism.
5. Vacuum explosion by strongly charged Black Hole
Ruffini (2000). Problems with formation of such strongly charged black hole.
6. GRB from superconducting strings,
Berezinsky et al., PR D (2001), 64, 043004
7. Transition from neutron star to quark star,
Berezhiani et al. astro-ph/02-09-257

About 4000 gamma ray bursts had been discovered
long and short GRB

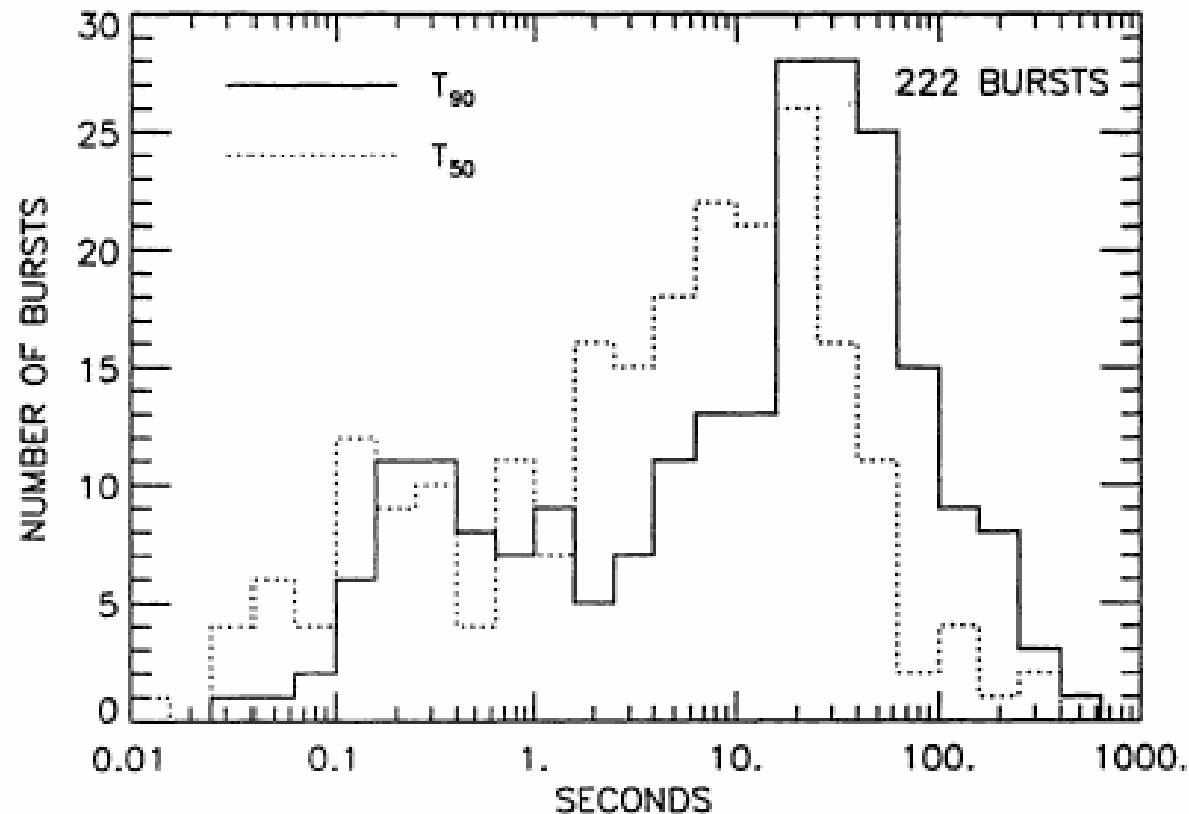


Figure 6 The duration distribution of 222 gamma-ray bursts from the BATSE catalog. Two separate measures are shown, representing 50% and 90% of the total burst fluence. A bimodal distribution is seen, with a separation near 2 s. (From Fishman et al 1994b.)

High redshifts, up to $Z \sim 6$, optical afterglows, GRB-SN connections – only by long GRB.

- Origin may be different (still not known for both types)

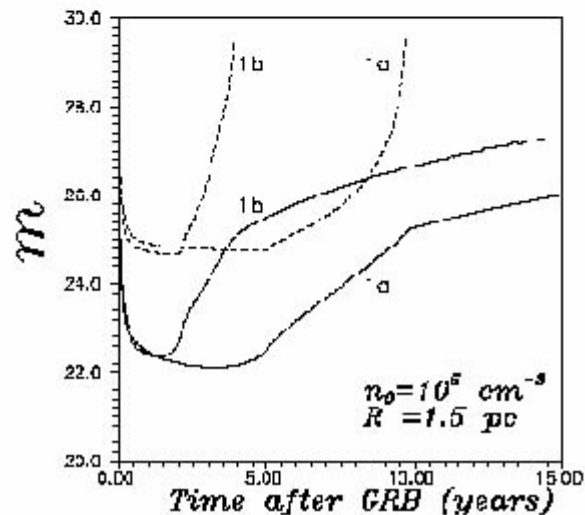
AFTERGLOW FROM THE HEATED GAS

The magnitudes of the counterparts (upper limit - solid line, lower limit - dashed line) as a function of time after burst for GRB with total flux near the Earth $F\{\text{GRB}\} = 10^{-4}$ erg/cm²:

1a. - for the case $E = 10^{52}$ erg; $n_0 = 10^5$ cm⁻³;

1b - for the case $E = 10^{51}$ erg; $n_0 = 10^5$ cm⁻³

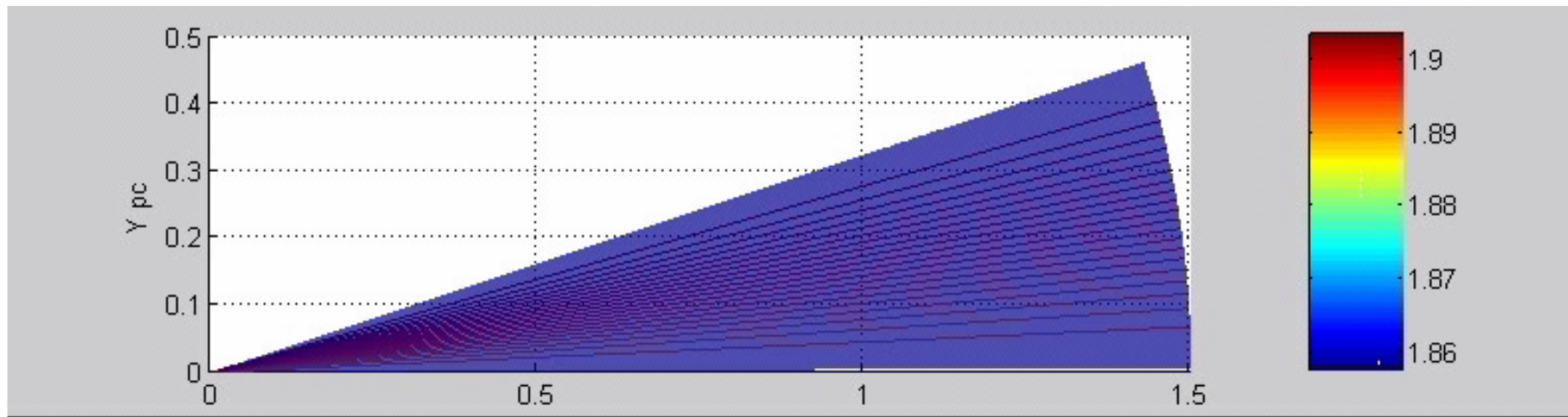
(B.-K., Timokhin, 1997)



Temperature distribution in the part of non-uniform cloud with $N_{\text{max}}=10^{-5}$,
(low-density cone)
in the cone after GRB with isotropic energy output 10^{52} erg, **Barkov (2004), PhD.**

$$\theta = \pi / 10$$

Barkov, Bisnovatyi-Kogan: astro/ph 0410186



GRB041219 - Infrared afterglow

Explosion in the dust:

- **INFRARED AFTERGLOW OF THE GAMMA RAY BURST AS THE RESULT**
- **OF RERADIATION FROM DUST IN A CIRCUMSTELLAR CLOUD**
- **M. V. Barkov and G. S. Bisnovatyi-Kogan**
- *Astrophysics, Vol. 48, No. 3, 2005*

Prompt Optical Emission.

GRB990123 about 100 s. T(50%)=30 s. T(90%)=63 s.

F(BATSE)= $5.1 \cdot 10^{-4}$ erg/cm²

ASCA 2-10 keV, 55 h, 10^{-12} erg/cm²/s

OSSE < 10MeV; COMPTEL 0.2-30 MeV (46 s.)

Beppo-SAX - Localization

Optics:

ROTSE, Los Alamos, t > 22.18 s after beginning of GRB

Unfiltered light

Jan 24, 40 min. KECK spectrum (optical)

Lines: Mg II, Si II, Fe II, Zn II, C IV, Al II, Fe II ...

Redshift: z=1.61 Q(gamma)> $2.3 \cdot 10^{54}$ erg

L(opt) > $2 \cdot 10^{16}$ Solar Luminosity = $8 \cdot 10^{49}$ erg/s

Radio: VLA 8.46 GHz about 260 microJansky;

Westerbork 4.88 GHz < 130 microJansky; Jan. 24.4, 15 GHz – NO FLUX

GRB 021004 (15m, z=2.3)

GRB 030329 (12.4m, z=0.168)

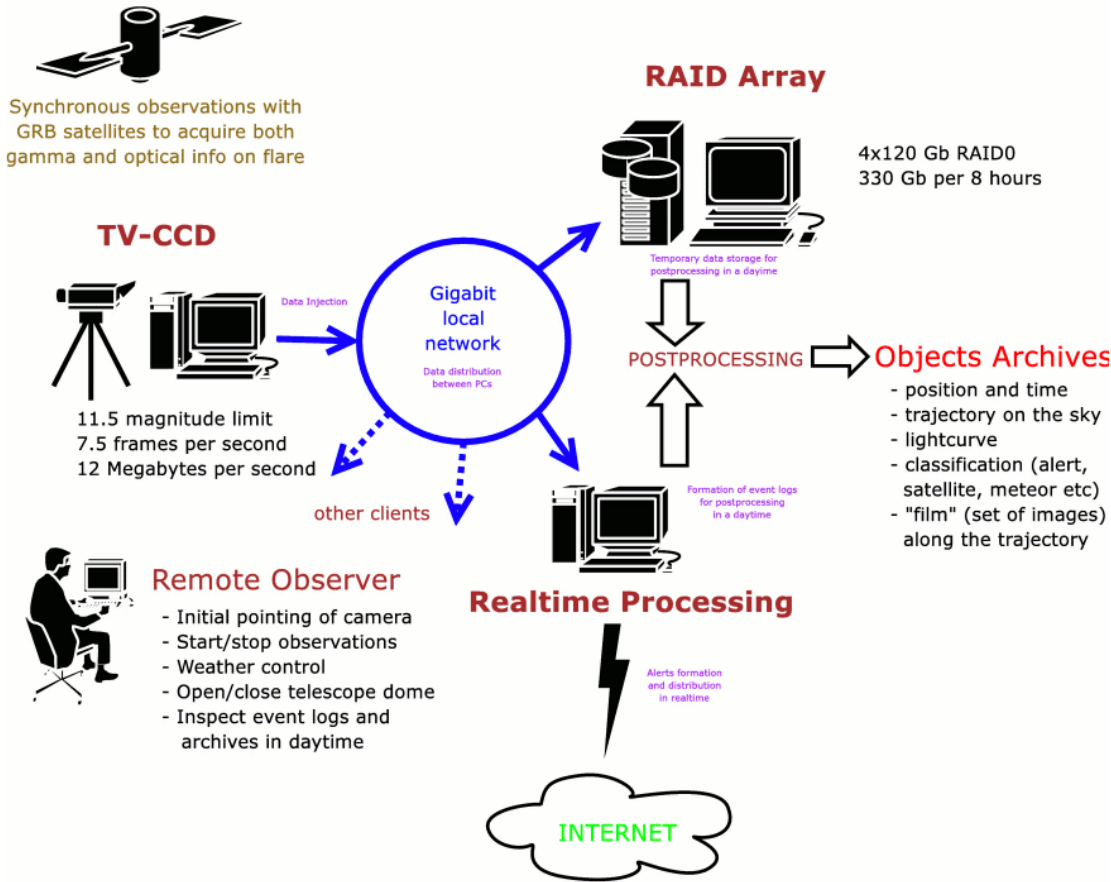
GRB 030418 (16.9m)

Search of rapid optical transients in wide fields

SAO

Field of view – 400-600 sq. grad
 Time resolution – 0.13 sec
 Limiting value – 10 – 11.5m

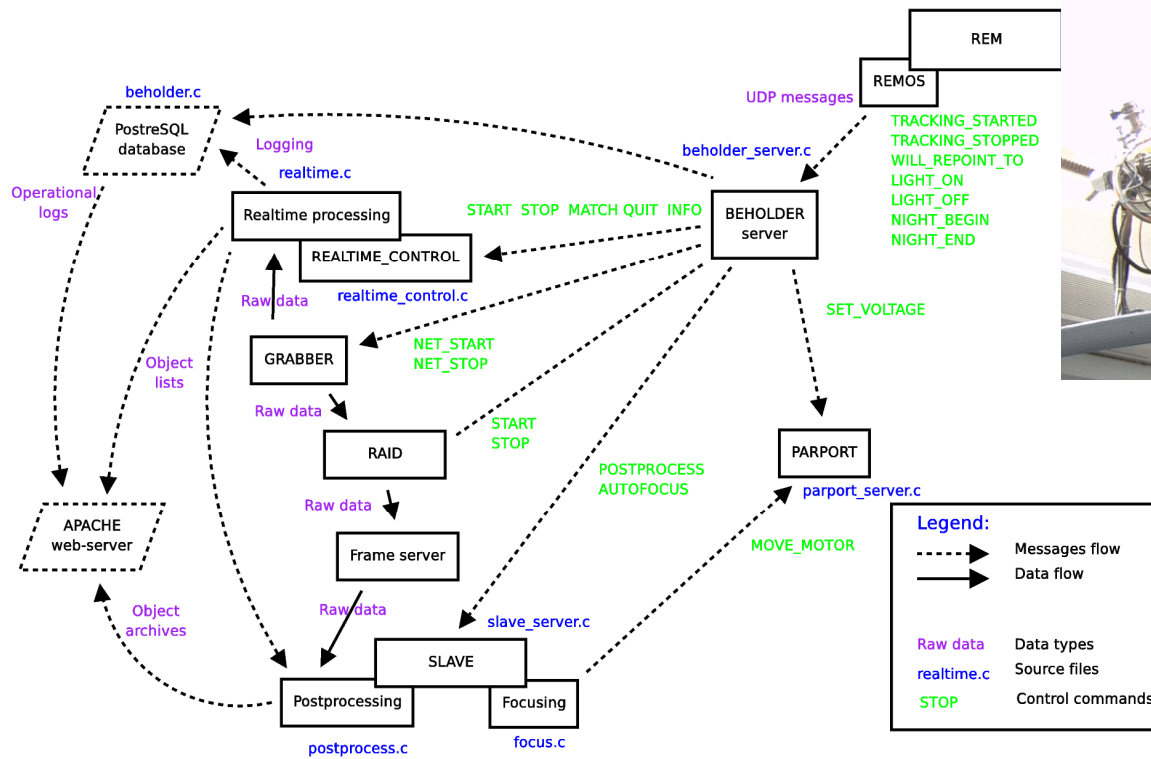
Amount of data – 600 Gb/night



Camera FAVOR - NIIPP, SAO, IKI

Pozanenko (IKI), Beskin (SAO), Bondar (NIIPP)

Data analysis in real time scale



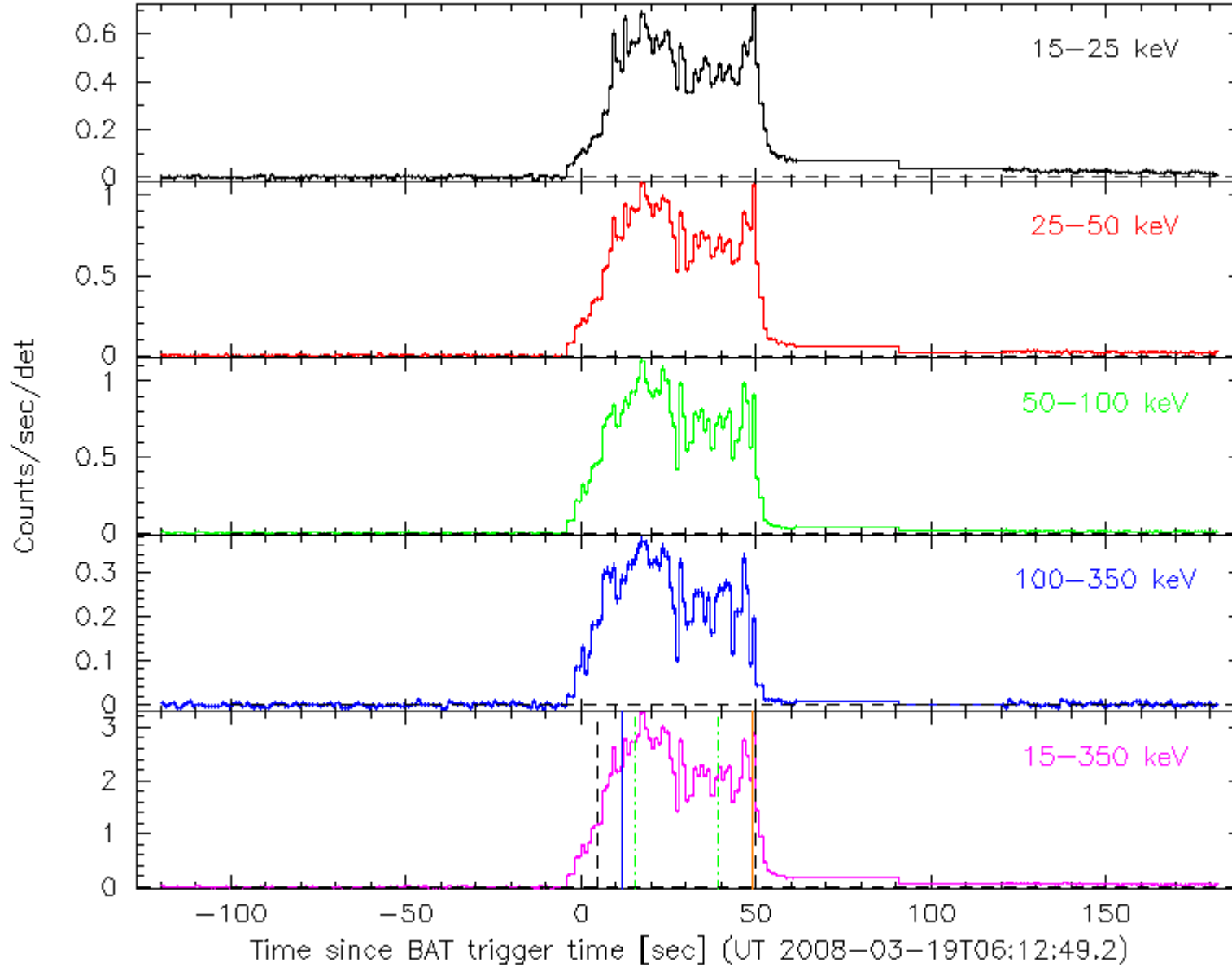
TORTOREM = Tortora + REM

La Silla,
In automatic regime since May, 2006

SWIFT

Swift-BAT GRB 319B

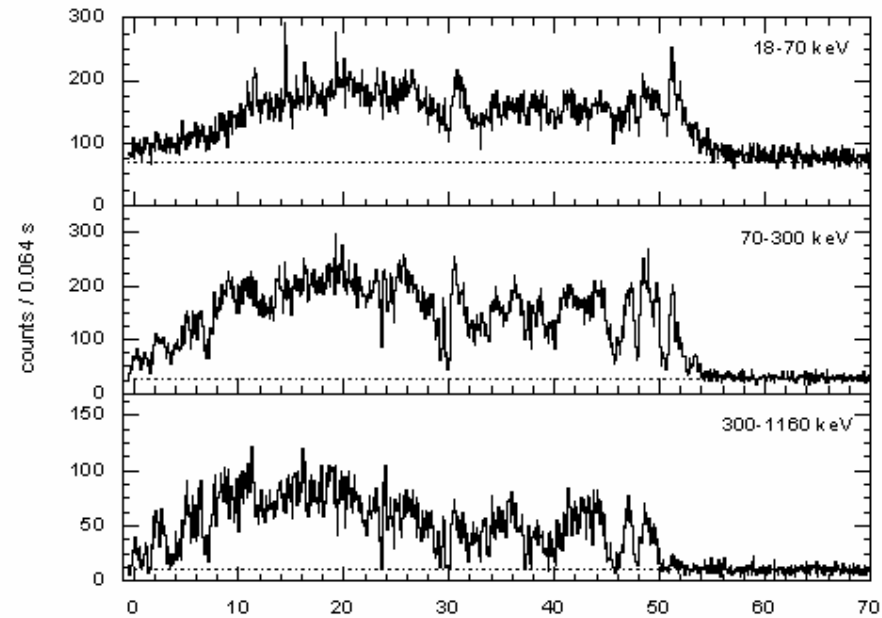
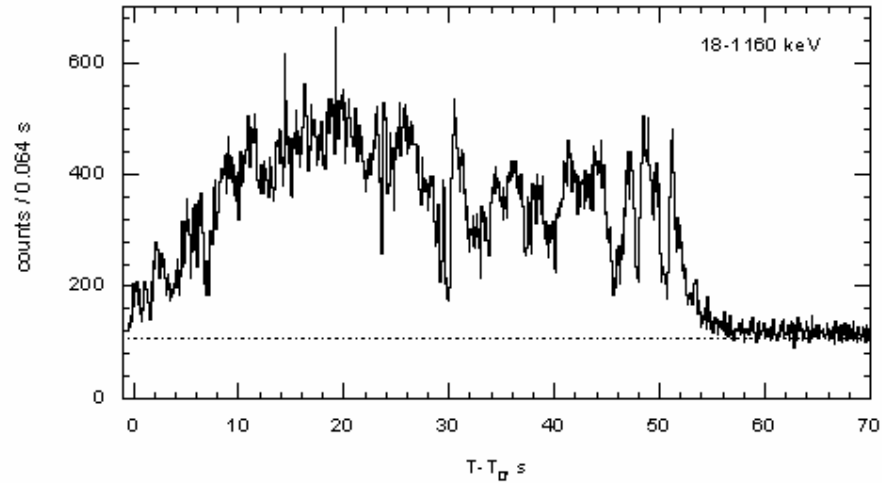
Maskweighted Lightcurve (1 s binning)



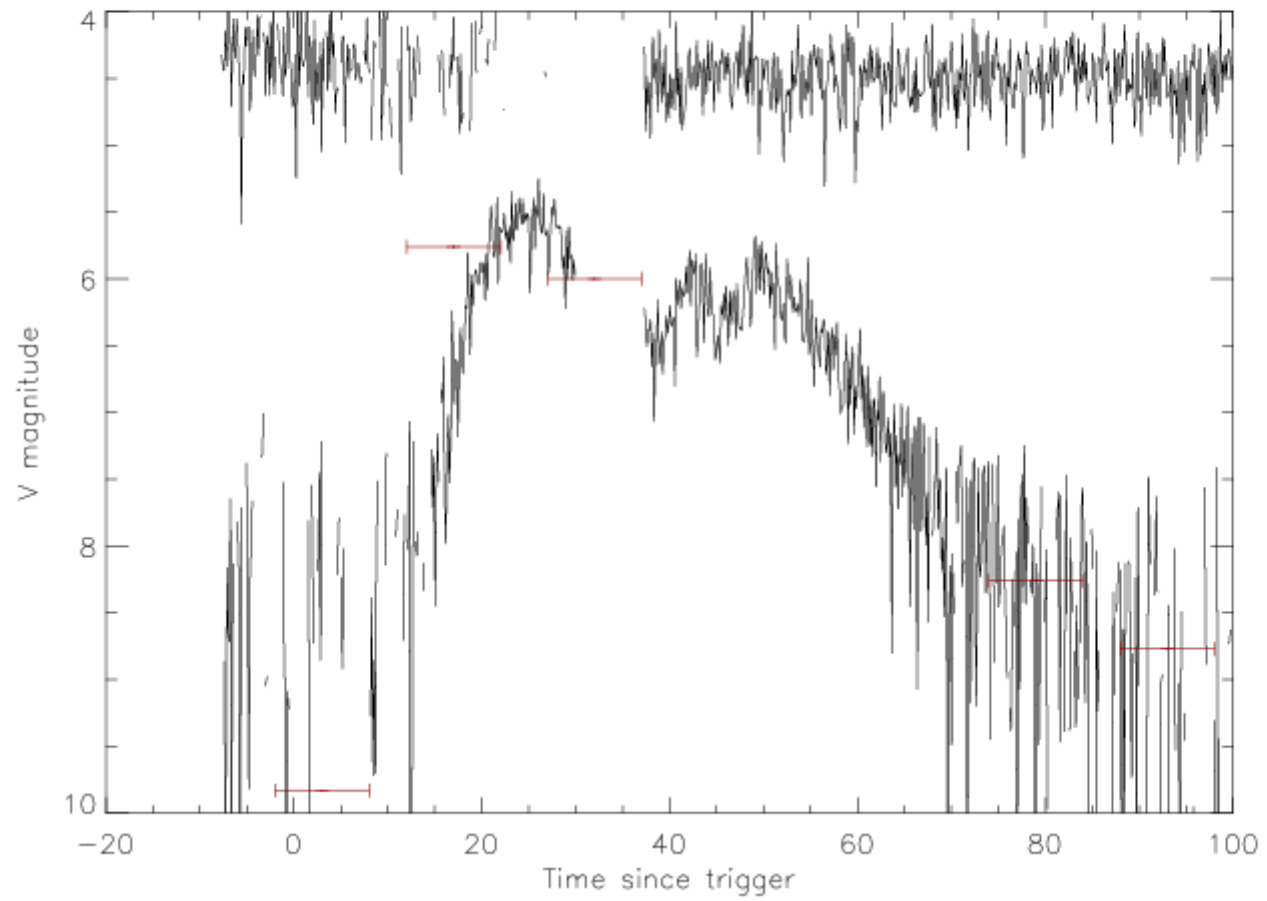
KONUS

KONUS-WIND GRB 080319
 $T_0 = 22370.339$ s UT (06:12:50.339)

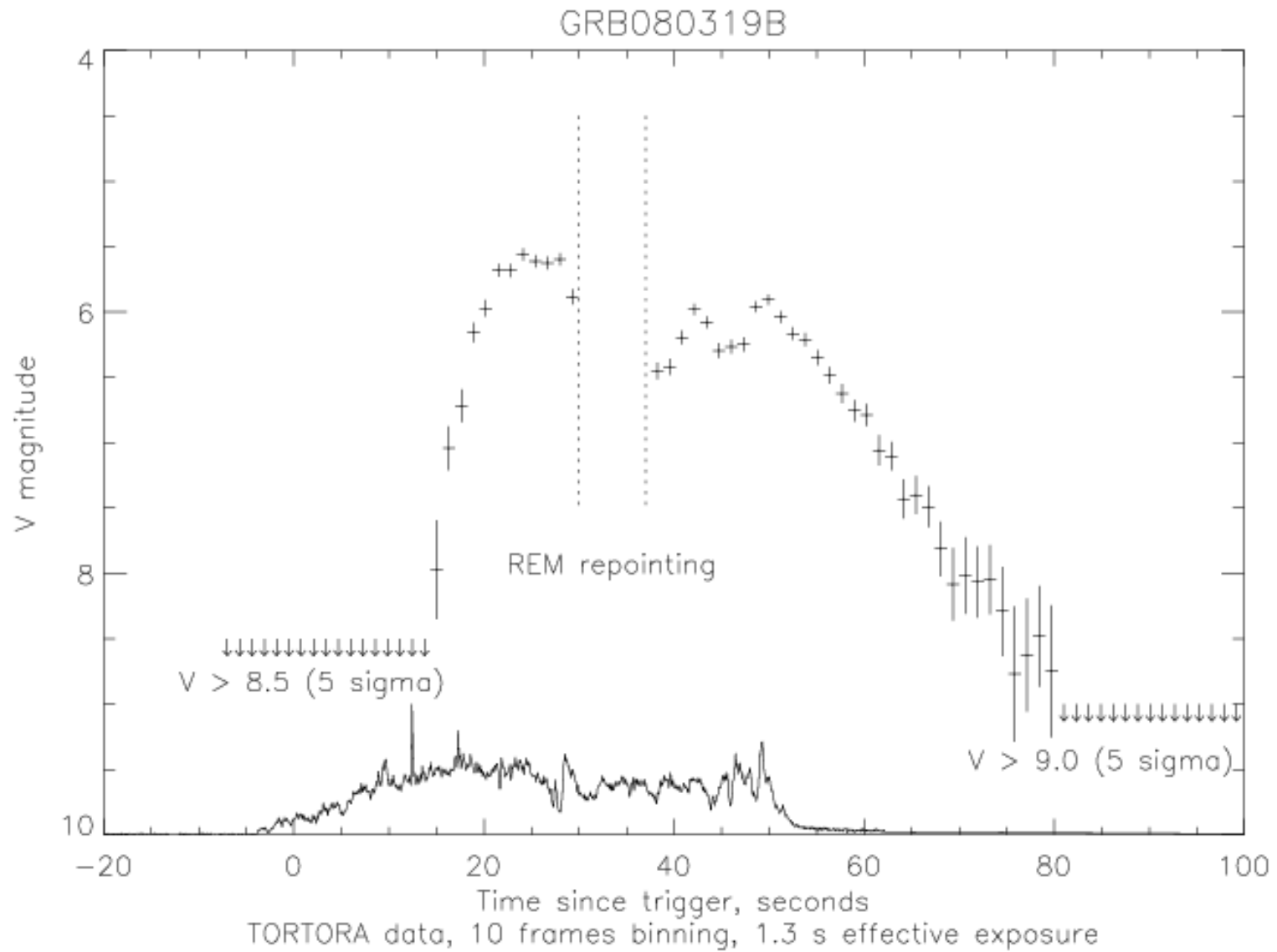
S2

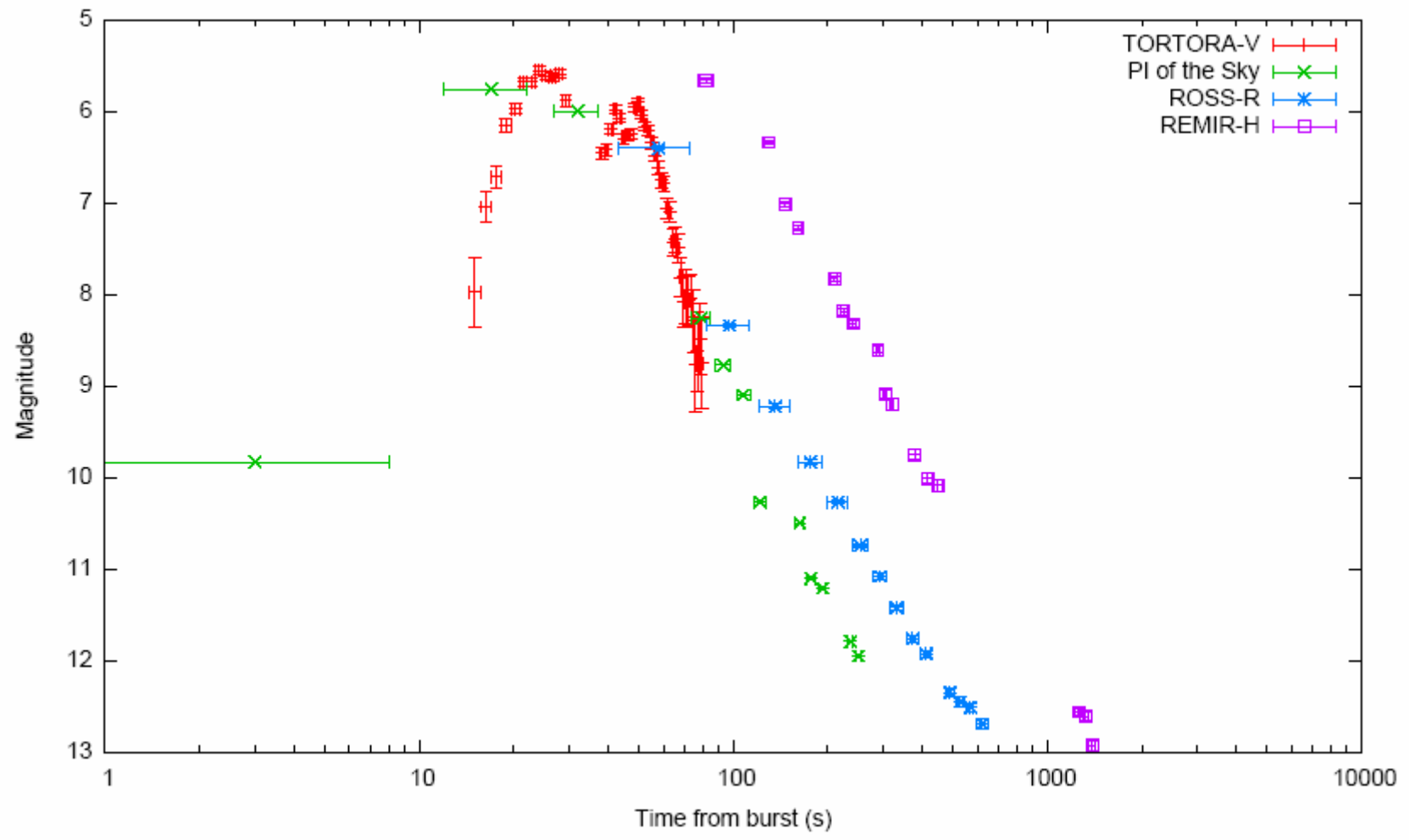


Tortora

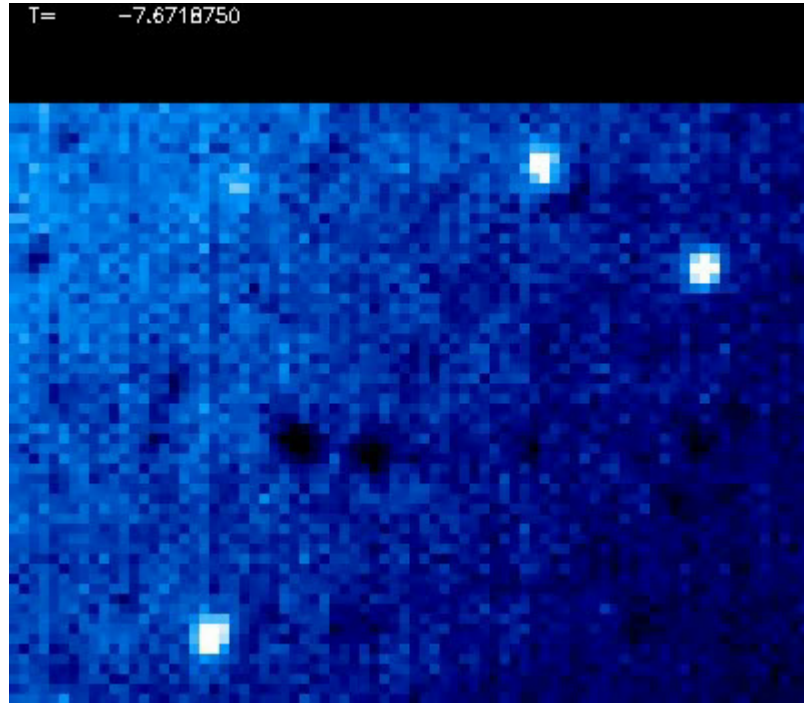


Tortora





T= -7.6718750



Prompt optical emission is strongly correlated with gamma

- May be it has the same collimation, as gamma radiation.
- Optical afterglows (at longer times) should not be collimated.

- **Giant bursts in SGR similar to short GRB**
- Mazets, E. P., et al. 1999b, *Astronomy Letters*, 25, 73
- Bisnovatyi-Kogan, G. S. 1999, preprint (astro-ph/9911275)

Short GRB, interpreted as giant bursts of SGR

In **M31 (Andromeda)** -1 February, 2007 (**~ 7 E46 erg**)

Mazets et al., arXiv:0712.1502

In **M81** - 3 November 2005 (**~ 1 E45 erg**) **Golenetskii et al. (2005) GCN..4197**

SGR: neutron stars with periods 5.16 – 8 seconds

Giant bursts, L in the peak increase 5 – 6 orders of magnitude

Slow rotation, low rotational energy, observed average luminosity exceeds rotational loss of energy more than 10 times, and orders of magnitude during giant outbursts

Suggestion: source of energy – magnetic field - magnetars

DISCOVERY OF TWO HIGH MAGNETIC FIELD RADIO PULSARS

F. CAMILO,^{1,2} V. M. KASPI,^{3,4,5} A. G. LYNE,² R. N. MANCHESTER,⁶ J. F. BELL,⁶ N. D'AMICO,^{7,8}
N. P. F. MCKAY,² AND F. CRAWFORD³

We report the discovery of two young isolated radio pulsars with very high inferred magnetic fields. PSR J1119–6127 has period $P = 0.407$ s, and the largest period derivative known among radio pulsars, $\dot{P} = 4.0 \times 10^{-12}$. Under standard assumptions these parameters imply a characteristic spin-down age of only $\tau_c = 1.6$ kyr and a surface dipole magnetic field strength of $B = 4.1 \times 10^{13}$ G. We have measured a stationary period second derivative for this pulsar, resulting in a braking index of $n = 2.91 \pm 0.05$. We have also observed a glitch in the rotation of the pulsar, with fractional period change $\Delta P/P = -4.4 \times 10^{-9}$. Archival radio imaging data suggest the presence of a previously uncataloged supernova remnant centered on the pulsar. The second pulsar, PSR J1814–1744, has $P = 3.975$ s and $\dot{P} = 7.4 \times 10^{-13}$. These parameters imply $\tau_c = 85$ kyr, and $B = 5.5 \times 10^{13}$ G, the largest of any known radio pulsar.

Both PSR J1119–6127 and PSR J1814–1744 show apparently normal radio emission in a regime of magnetic field strength where some models predict that no emission should occur. Also, PSR J1814–1744 has spin parameters similar to the anomalous X-ray pulsar (AXP) 1E 2259+586, but shows no discernible X-ray emission. If AXPs are isolated, high magnetic field neutron stars (“magnetars”), these results suggest that their unusual attributes are unlikely to be merely a consequence of their very high inferred magnetic fields.

PSR J1847–0130: A RADIO PULSAR WITH MAGNETAR SPIN CHARACTERISTICS

M. A. McLAUGHLIN,¹ I. H. STAIRS,² V. M. KASPI,³ D. R. LORIMER,¹ M. KRAMER,¹ A. G. LYNE,¹ R. N. MANCHESTER,
F. CAMILO,⁵ G. HOBBS,⁴ A. POSSENTI,⁶ N. D’AMICO,^{7,8} AND A. J. FAULKNER¹

We report the discovery of PSR J1847–0130, a radio pulsar with a 6.7 s spin period, in the Parkes Multibeam Pulsar Survey of the Galactic plane. The slowdown rate for the pulsar, $1.3 \times 10^{-12} \text{ s s}^{-1}$, is high and implies a surface dipole magnetic field strength of $9.4 \times 10^{13} \text{ G}$. This inferred dipolar magnetic field strength is the highest by far among all known radio pulsars and over twice the “quantum critical field” above which some models predict radio emission should not occur. The inferred dipolar magnetic field strength and period of this pulsar are in the same range as those of the anomalous X-ray pulsars, which have been identified as being “magnetars” whose luminous X-ray emission is powered by their large magnetic fields. We have examined archival *ASCA* data and place an upper limit on the X-ray luminosity of J1847–0130 that is lower than the luminosities of all but one anomalous X-ray pulsar. The properties of this pulsar prove that inferred dipolar magnetic field strength and period cannot alone be responsible for the unusual high-energy properties of the magnetars and create new challenges for understanding the possible relationship between these two manifestations of young neutron stars.

Two Radio Pulsars with Magnetar Fields

Abstract. PSRs J1847–0130 and J1718–37184 have inferred surface dipole magnetic fields greater than those of any other known pulsars and well above the “quantum critical field” above which some models predict radio emission should not occur. These fields are similar to those of the anomalous X-ray pulsars (AXPs), which growing evidence suggests are “magnetars”. The lack of AXP-like X-ray emission from these radio pulsars (and the non-detection of radio emission from the AXPs) creates new challenges for understanding pulsar emission physics and the relationship between these classes of apparently young neutron stars.

Both of these pulsars were discovered in the Parkes Multibeam Pulsar Survey (see e.g. Manchester et al. 2001). PSR J1847–0130 has a spin period of 6.7 s and inferred surface dipole magnetic field¹ of 9.4×10^{13} G. PSR J1718–37184 has a period of 3.4 s and magnetic field of 7.4×10^{13} G. The magnetic fields of both pulsars are well above the “quantum critical field” $\simeq 4.4 \times 10^{13}$ G above which some models predicted radio emission should not occur (Baring & Harding 1998).

A radio pulsar with an 8.5-second period that challenges emission models

Young, M. D.; Manchester, R. N.; Johnston, S.

Nature, Volume 400, Issue 6747, pp. 848-849 (1999).

Radio pulsars are rotating neutron stars that emit beams of radiowaves from regions above their magnetic poles. Popular theories of the emission mechanism require continuous electron-positron pair production, with the potential responsible for accelerating the particles being inversely related to the spin period. Pair production will stop when the potential drops below a threshold, so the models predict that radio emission will cease when the period exceeds a value that depends on the magnetic field strength and configuration. Here we show that the pulsar J2144-3933, previously thought to have a period of 2.84s, actually has a **period of 8.51s**, which is by far the longest of any known radio pulsar. Moreover, under the usual model assumptions, based on the neutron-star equations of state, this slowly rotating pulsar should not be emitting a radio beam. Therefore either the model assumptions are wrong, or **current theories of radio emission must be revised.**

Pulsar Astronomy - 2000 and Beyond, ASP Conference Series, Vol. 202; Proc. of the 177th Colloquium of the IAU held in Bonn, Germany, 30 August - 3 September 1999

Young, M. D.; Manchester, R. N.; Johnston, S.

Ha, ha, ha, ha, staying alive, staying alive: A radio pulsar with an 8.5-s period challenges emission models.

SGR: Soft Gamma Repeaters

3 objects inside the Galaxy

SGR 1900+14, discovered by Mazets et al.(1979)

(**Giant burst at 27 August 1998, $>7 E43$ erg**)

SGR 1806-20, observed by Mazets et al. (1980); identified as SGR by Laros et al. (1986) (**Giant burst at 27 December 2006, $\sim 2 E46$ erg**)

SGR 1627-41, discovered by BATSE

(**semi-giant burst at 18 June 1998, $\sim 1 E43$ erg**)

1 in Large Magelanic Cloud: **SGR 0526-66**, discovered by Mazets et al.(1979)

(**Giant burst at 5 March 1979, $>2 E44$ erg**)

Short GRB, interpreted as giant bursts of SGR

In **M31 (Andromeda)** -1 February, 2007 (**$\sim 7 E46$ erg**) Mazets et al., arXiv:0712.1502

In **M81** - 3 November 2005 (**$\sim 1 E45$ erg**) Golenetskii et al. (2005) GCN..4197

Soft Gamma Repeaters (SGR)

Mazets et al., *AZhLett*, **5**, 1979, 641-643

Soft gamma-ray bursts from the source B1900+14

AZhLett, **5**, 1979, 636-640

Recurrent gamma-ray bursts from the flaring source FXP 0520 - 66

19.01

STATISTICAL PROPERTIES OF THE SOFT GAMMA
REPEATER(SGR) GB790107

J. G. Laros, E. E. Fenimore, R. W. Klebesadel
(Los Alamos), and S. R. Kane (UCB)

The high energy transient GR790107, originally cataloged as a gamma-ray burster by Mazets, et al., has recently been shown to be repetitive, with the highest activity (~80 out of ~100 events) seen in late 1983 (Laros, et al. 1986, Nature, 322, 152). Its mean photon energy of ~30 KeV, together with the repetitive behavior, impel us to place it in a new class, which we tentatively call soft gamma repeaters (SGRs). Other probable SGRs are GB790324 and possibly the "March 5" source GB790305B. Preliminary data on the repetitions of GB790107 were presented at the Toulouse COSPAR meeting and at the Taos Gamma-Ray Stars conference. The repetitions, with ~0.2 S durations and ~30 KeV characteristic energies, appear very similar to the first detected outburst in 1979. Using data from the UCB/Los Alamos experiment on ICE, we have determined other characteristics of the repetitions, namely: (1) The interval between successively observed events ranges from seconds to years, (2) There is little correlation between the interval and the intensity of the preceding or following outburst, (3) No periodicities are evident, (4) The luminosities of the repetitions ranged from $\sim 1 \times 10^{-7}$ (The instrumental threshold) to $\sim 3 \times 10^{-6}$ ergs cm^{-2} , with the distribution monotonically falling with increasing luminosity. We will discuss these and other results on this intriguing new type of repeating high energy transient. This work was supported by the US DOE and NASA.

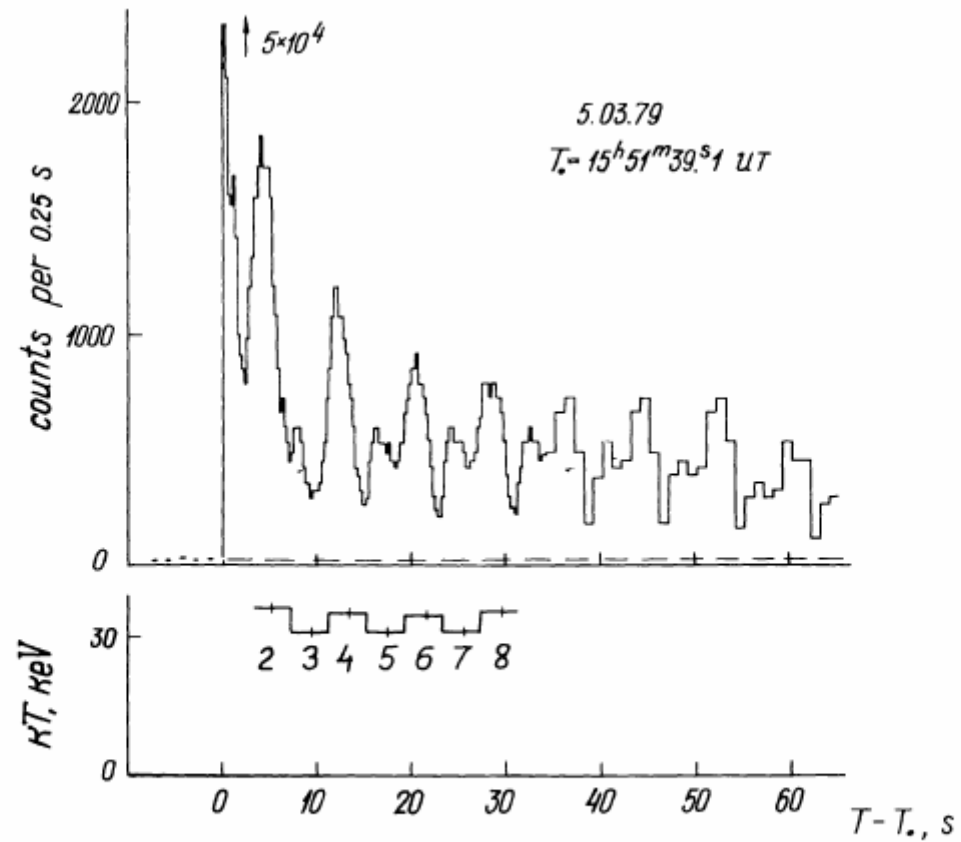


Fig. 1. 5 March 1979 gamma-ray burst. Top: time profile; narrow initial pulse and pulsations, resolution 0.25 s. Bottom: temperature variations for the thermal bremsstrahlung spectra in the pulsating stage of the burst, $I \propto \exp(-E/kT)$, time taken to measure each spectrum 4 s.

Mazets et al., 1981

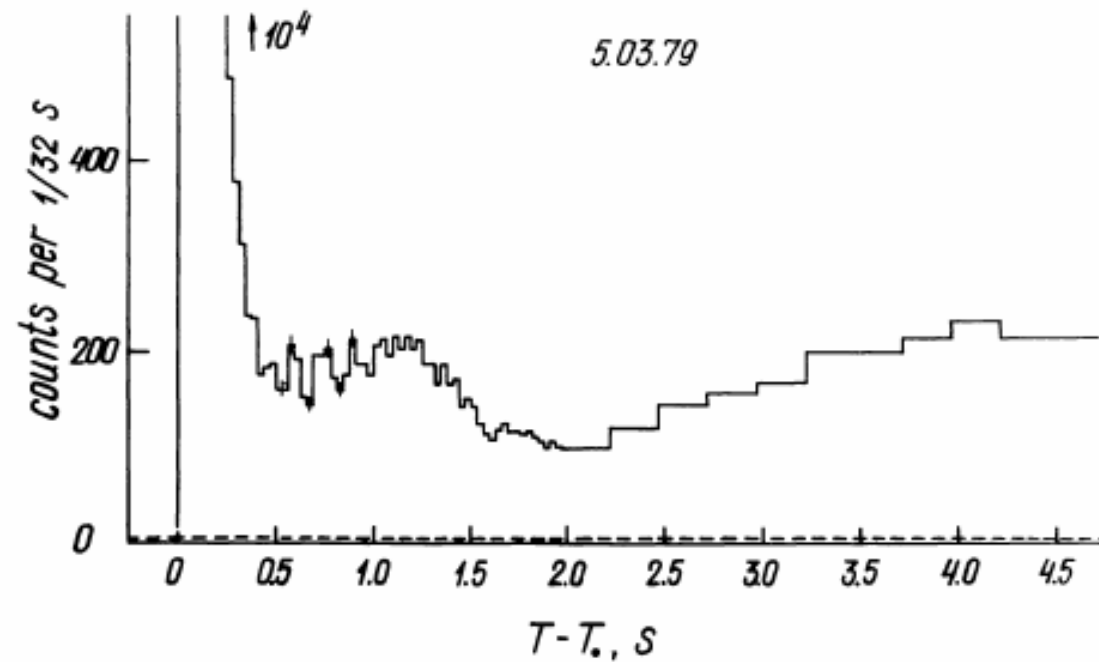
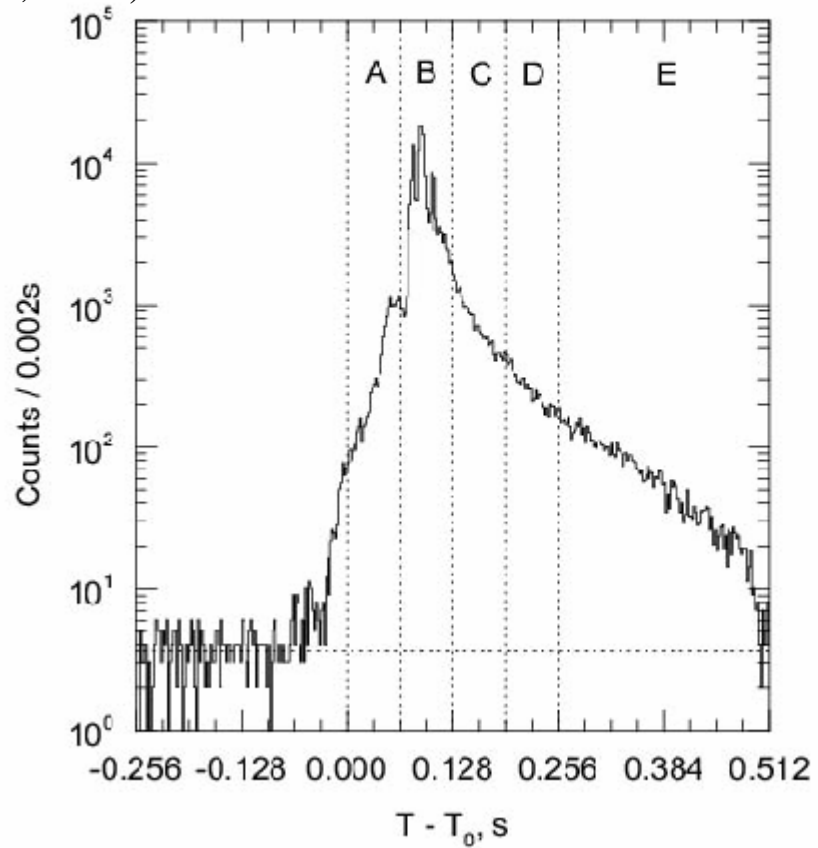


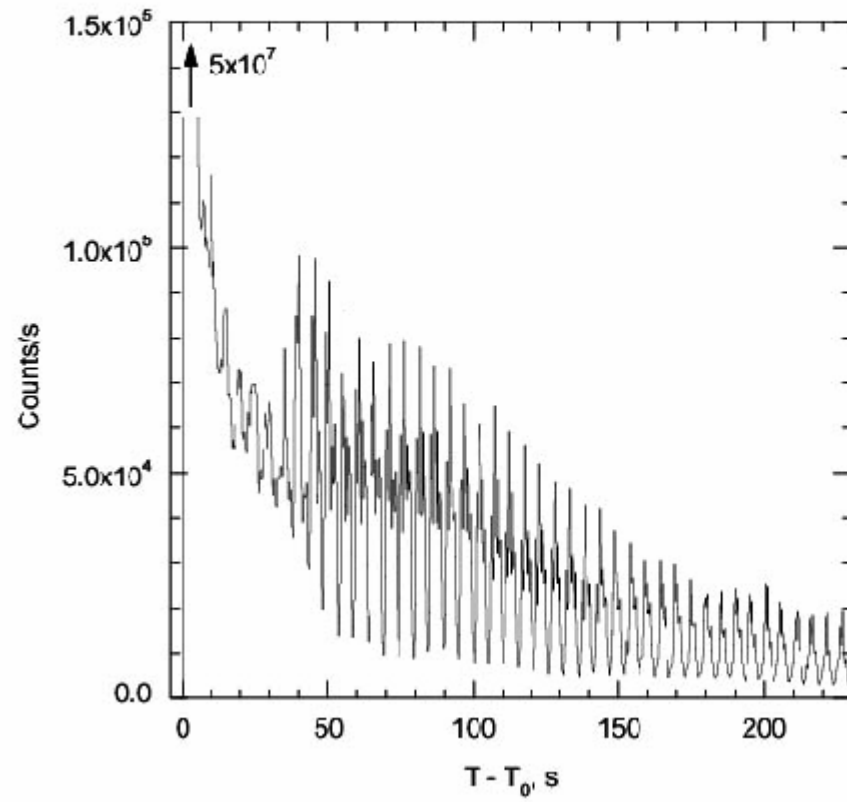
Fig. 4. The initial stage in the 5 March 1979 gamma burst. The maximum in the region $T - T_0 = 0.5-1.5$ s does not belong to the pulsation series with the period 8.1 ± 0.1 s. In the interval 0.4–1.2 s, fast oscillations are superimposed on a relatively-smooth intensity profile.

Mazets et al., 1981

The time history of the giant burst from the soft gamma repeater SGR 1627-41. on June 18, 6153 s UT corrected for dead time. Photon energy $E > 15$ keV. The rise time is about 100 ms (Mazets, 1999a).

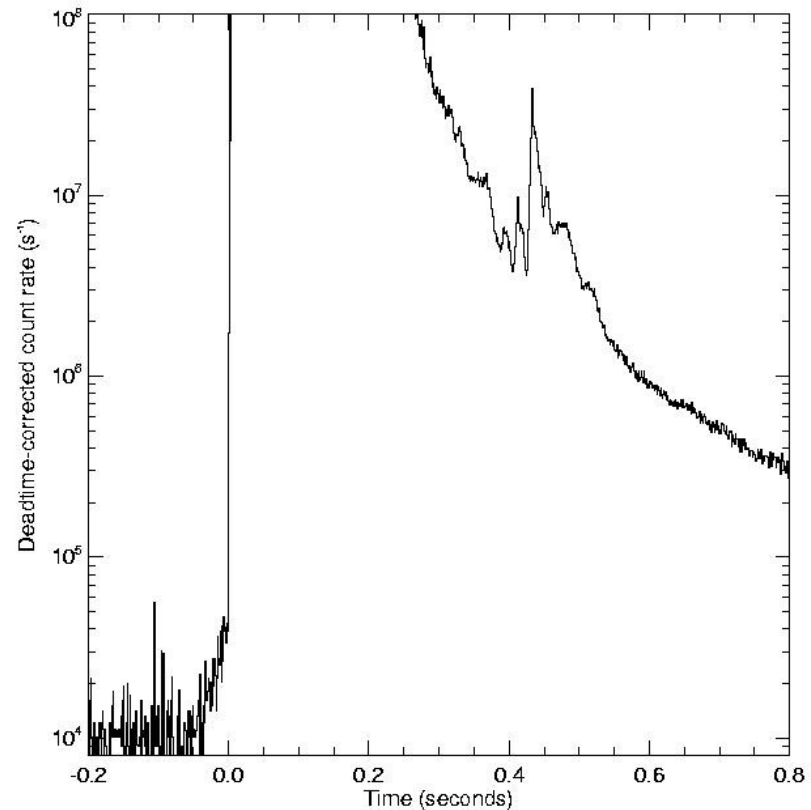


The giant 1998 August 27 outburst of the soft gamma repeater SGR 1900 + 14. Intensity of the $E > 15$ keV radiation (Mazets, 1999c).

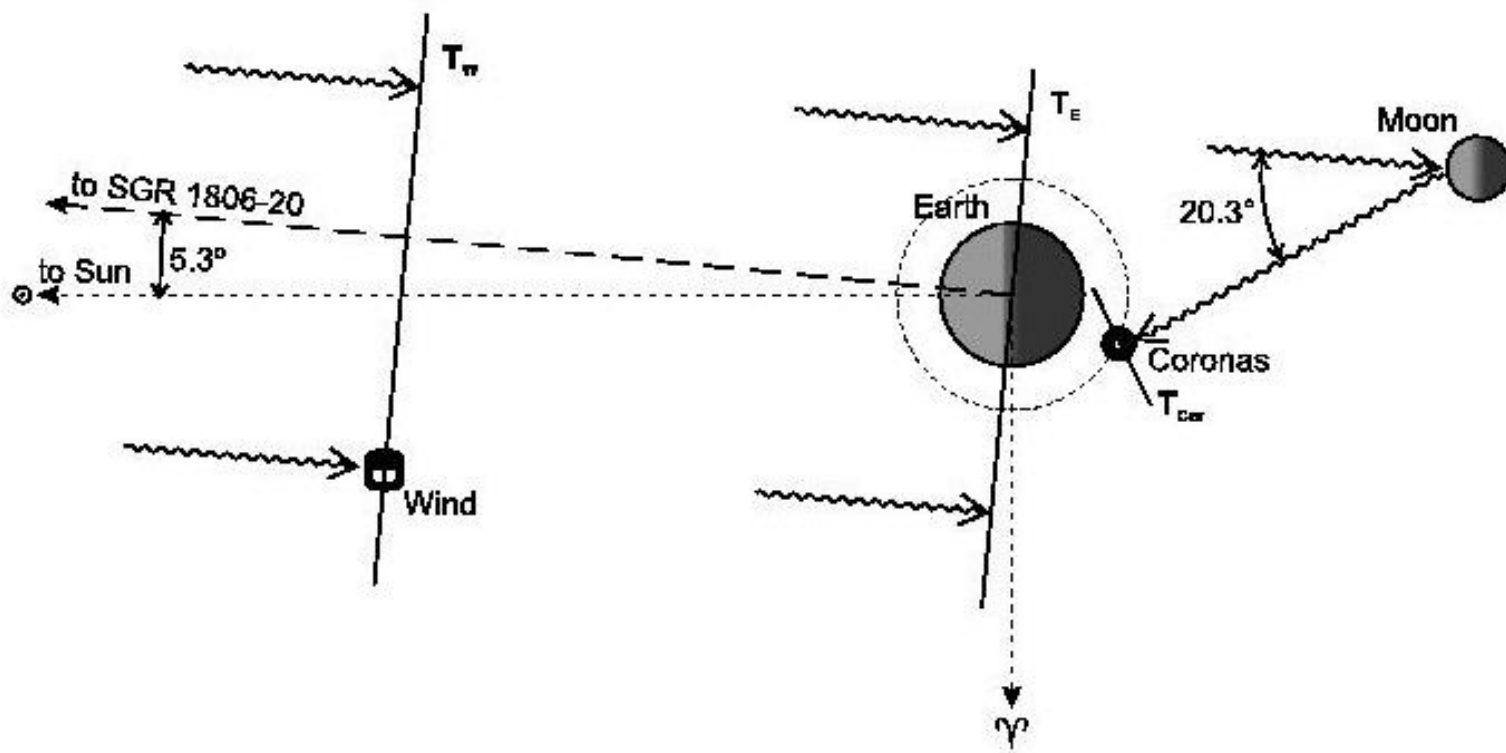


The greatest flare of a Soft Gamma Repeater

- On December 27 2004 the greatest flare from SGR 1806-20 was detected by many satellites: Swift, RHESSI, Konus-Wind, Coronas-F, Integral, HEND, ...
- 100 times brighter than ever!

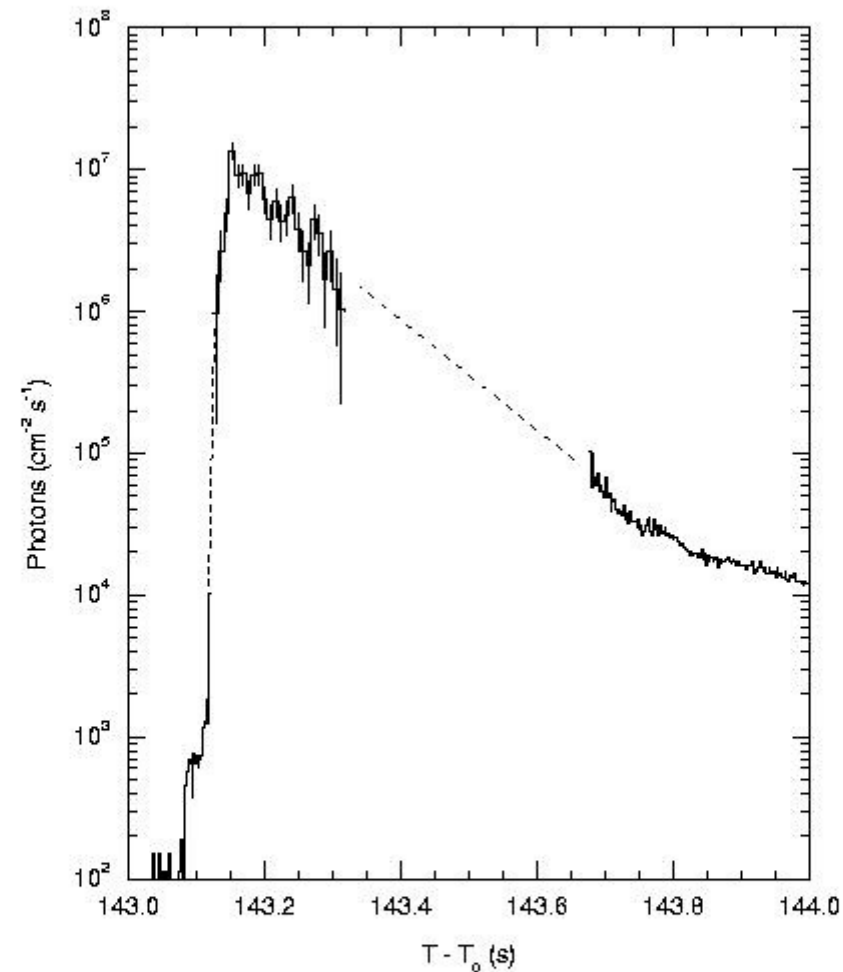


Palmer et al.
Astro-ph/0503030



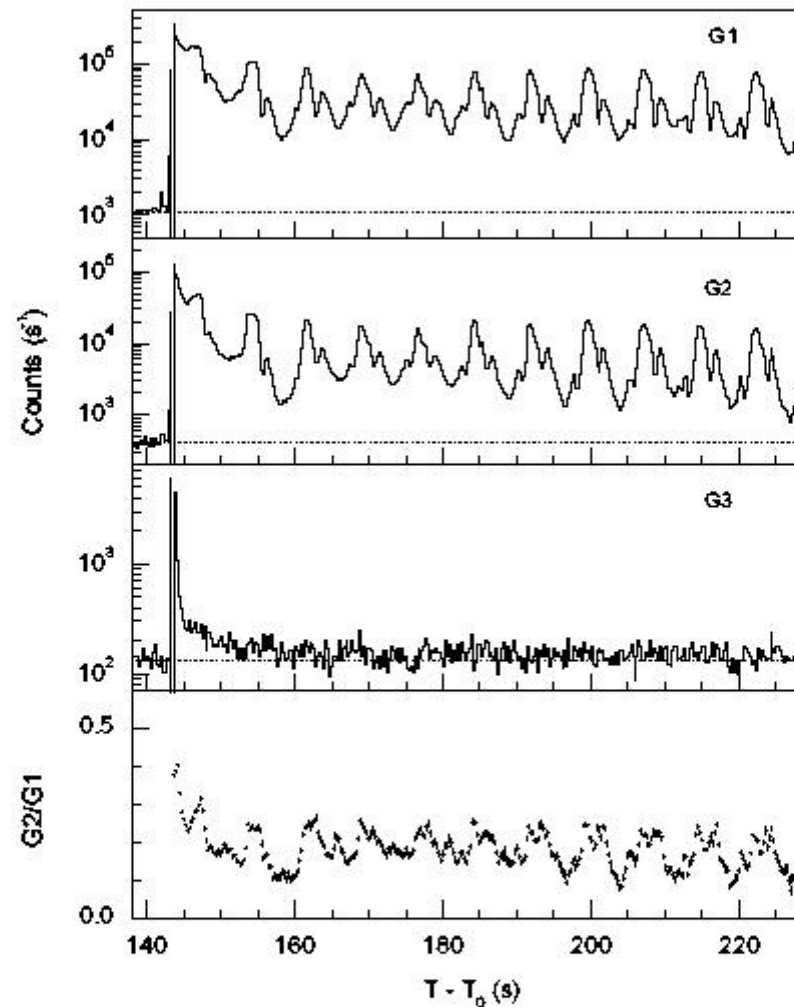
2004 December 27
giant outburst.

Reconstructed time history of the initial pulse. The upper part of the graph is derived from Helicon data while the lower part represents the Konus-Wind data. The dashed lines indicate intervals where the outburst intensity still saturates the Konus-Wind detector, but is not high enough to be seen by the Helicon.



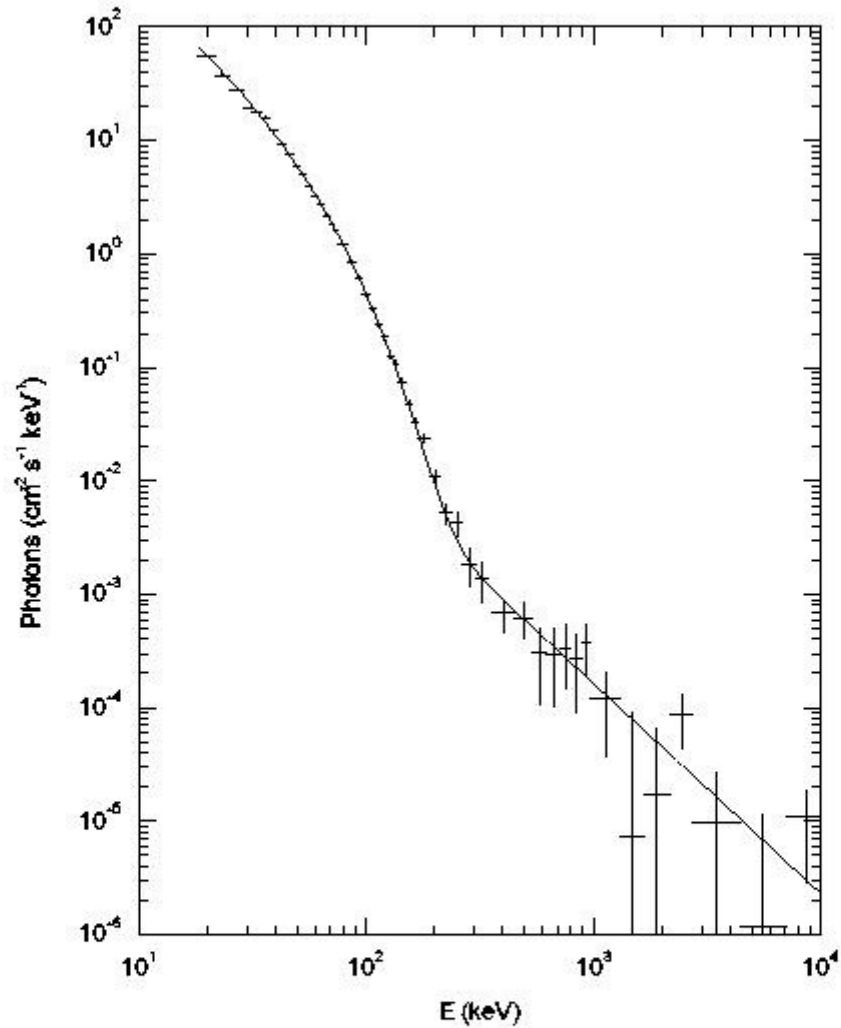
Mazets et al., 2005

Time history of the 2004 December 27 giant outburst recorded by the Konus-Wind detector in three energy windows G1 (16.5--65 keV), G2 (65--280 keV), and G3 (280--1060 keV), and the hardness ratio G2/G1. The moderate initial count rate growth to 10^2 -- 10^3 counts s^{-1} transforms rapidly to an avalanche-type rise to levels $>5 \times 10^7$ counts s^{-1} , which drives the detector to deep saturation for a time $\Delta T \simeq 0.5$ s. After the initial pulse intensity has dropped to $\sim 10^6$ counts s^{-1} , the detector resumes operation to record the burst tail.



Mazets et al., 2005

A spectrum of the burst tail averaged over the pulsation period. The low-energy component is similar to spectra of SGR's recurrent bursts with $E_0 \simeq 30$ keV. At high energies it exhibits a hard power-law component with $\alpha = -1.8 \pm 0.2$. This two-component model is shown by the solid line.



Mazets et al., 2005

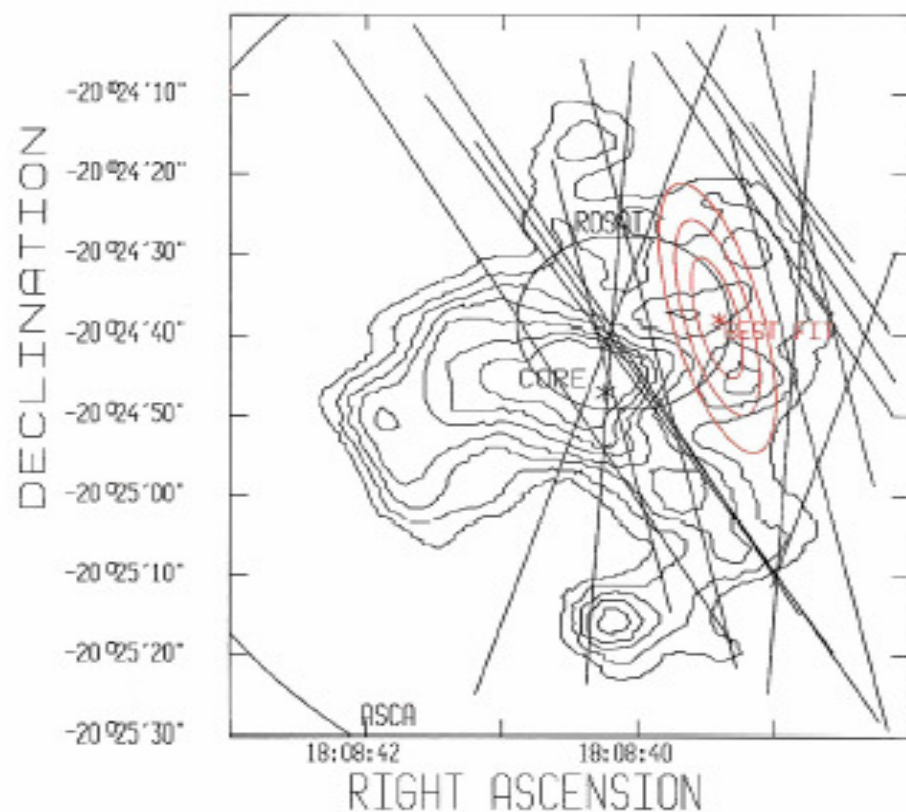


FIG. 2.—Eight IPN annuli (*black lines*) and the 1, 2, and 3 σ equivalent confidence contours (*red annuli*) for SGR 1806–20. The best-fit position and the position of the nonthermal core are indicated. The *ASCA* error circle is just visible in the lower left-hand and upper left-hand corners; its radius is 1', quoted as a systematic error, with no confidence limit given (Murakami et al. 1994). The *ROSNAT* PSPC error circle is at the center; its radius is 11", with no confidence limit quoted (Cooke et al. 1993). We have reanalyzed the *ROSNAT* data and confirm the presence of a weak source at this position, but we are unable to establish confidence limits for its position. The 3.6 cm radio contours of G10.0-0.3 are also shown, from Vasisht, Frail, & Kulkarni (1995).

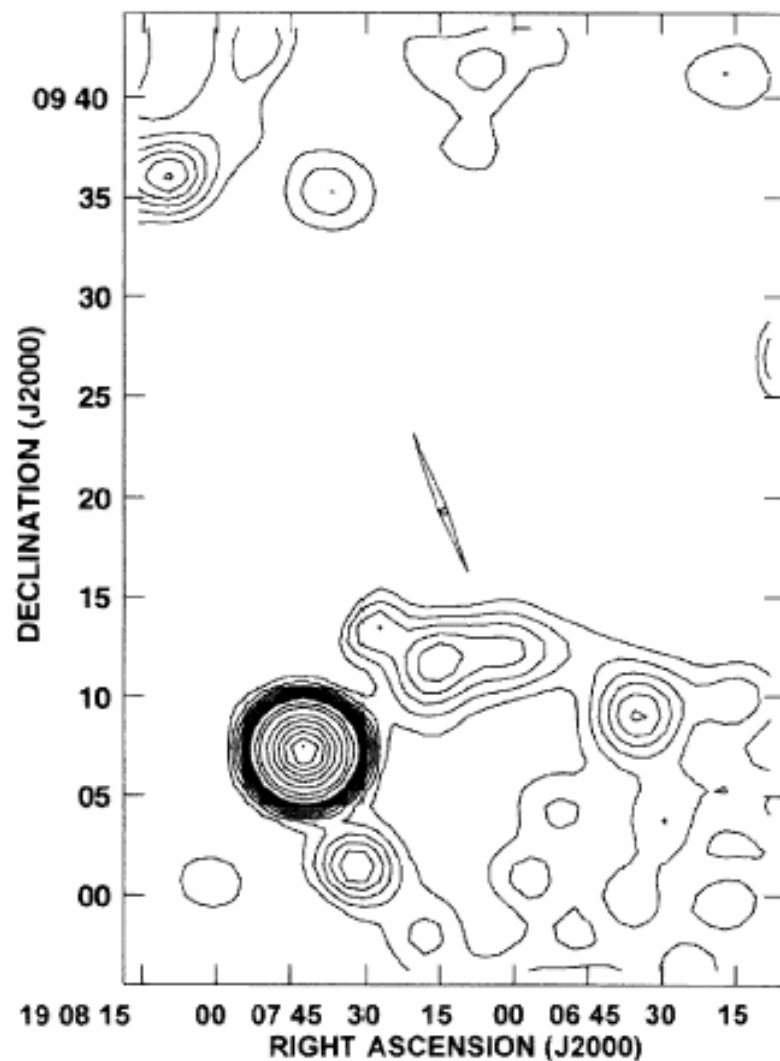


FIG. 2.—Error box for SGR 1900+14 superposed on a radio map of this region. The radio continuum image was taken at the VLA on 1994 February 7 at a frequency of 327 MHz (Vasisht et al. 1994). The synthesized beam size is approximately $3'$. The contour levels progress in steps of 20–200 mJy beam $^{-1}$. The higher contour levels progress in steps of 20 mJy beam $^{-1}$ to the peak of 1.6 Jy. The position of the *ROSAT* source within the error box is indicated.

SGR model: Magnetar $B=10^{14} - 10^{15}$ Gs

Magnetic Field Limit on SGR 1900+14

Rothschild, R. E.; Marsden, D.; Lingenfelter, R. E.

preprint arXiv:astro-ph/9911238

Astrophysical Journal, Volume 520, pp. L107-L110

We measured the period and spin-down rate for SGR 1900+14 during the quiescent period two years before the recent interval of renewed burst activity. We have shown that the spin-down age of SGR 1900+14 is consistent with a braking index of ~ 1 which is appropriate for wind torques and not magnetic dipole radiation. We have shown that a combination of dipole radiation, and wind luminosity, coupled with estimated ages and present spin parameters, imply that the magnetic field for SGR 1900+14 is less than 6×10^{13} G and that the efficiency for conversion of wind luminosity to x-ray luminosity is $< 2\%$.

Formation of very strongly magnetized neutron stars - Implications for gamma-ray bursts

Duncan, Robert C.; Thompson, Christopher

Astrophysical Journal, Part 2 - Letters, vol. 392, no. 1, June 10, 1992, p. L9-L13.

It is proposed that the main observational signature of magnetars, high-field neutron stars, is gamma-ray bursts powered by their vast reservoirs of magnetic energy. If they acquire large recoils, most magnetars are unbound from the Galaxy or reside in an extended, weakly bound Galactic corona. There is evidence that the soft gamma repeaters are young magnetars. It is argued that a convective dynamo can also generate a very strong dipole field after the merger of a neutron star binary, but only if the merged star survives for as long as about 10-100 ms. Several mechanisms which could impart a large recoil to these stars at birth, sufficient to escape from the Galactic disk, are discussed.

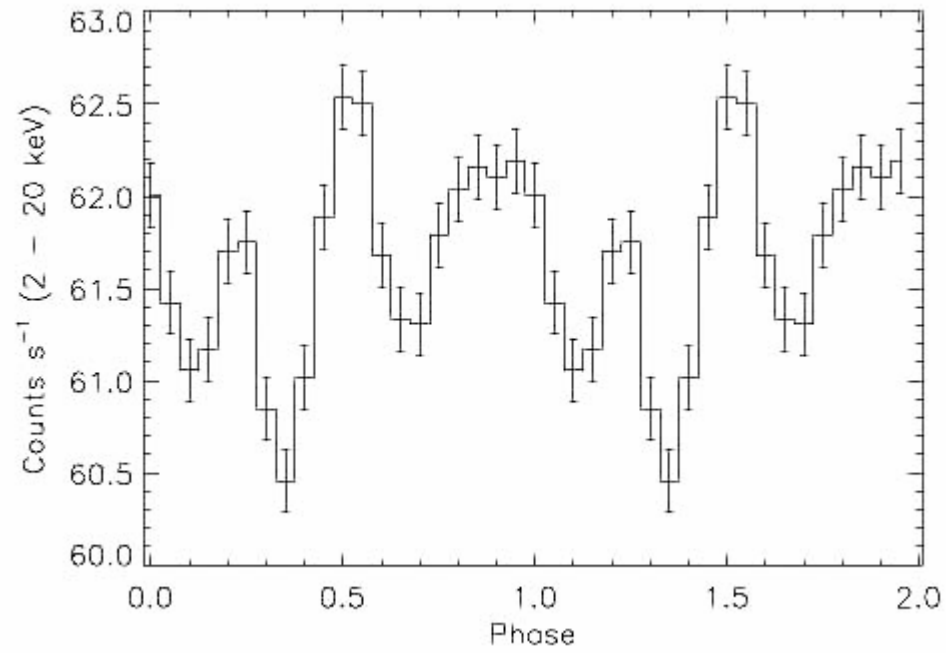
The soft gamma repeaters as very strongly magnetized neutron stars - I. Radiative mechanism for outbursts

Duncan, Robert C.; Thompson, Christopher

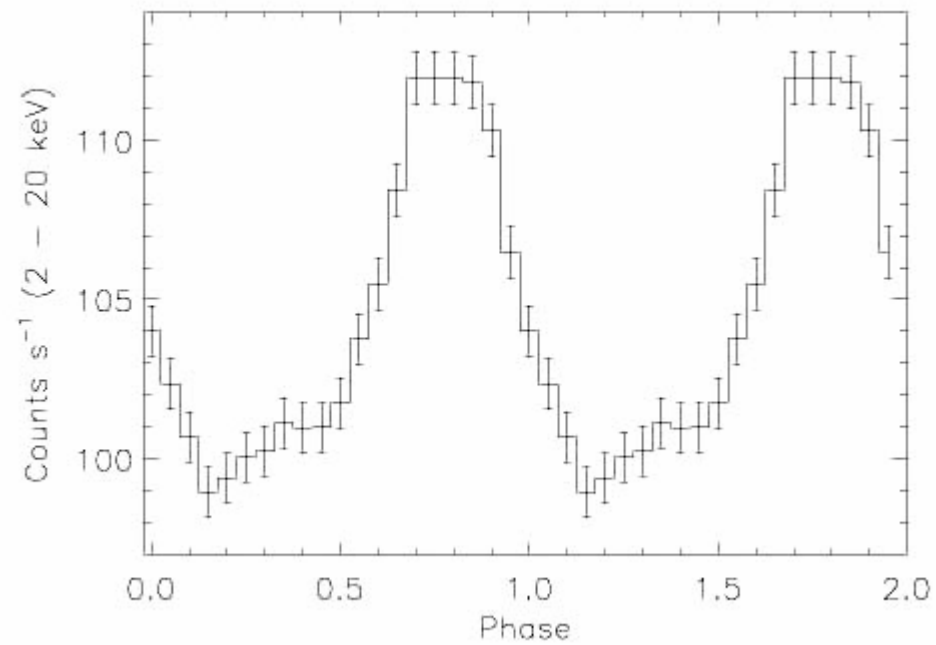
MN RAS, Volume 275, Issue 2, pp. 255-300 (1995) .

A radiative model for the soft gamma repeaters and the energetic 1979 March 5 burst is presented. We identify the sources of these bursts with neutron stars the external magnetic fields of which are much stronger than those of ordinary pulsars. Several independent arguments point to a neutron star with $B_{\text{dipole}} \sim 5 \times 10^{14}$ G as the source of the March 5 event. A very strong field can (i) spin down the star to an 8-s period in the $\sim 10^4$ -yr age of the surrounding supernova remnant N49; (ii) provide enough energy for the March 5 event; (iii) undergo a large-scale interchange instability the growth time of which is comparable to the ~ 0.2 -s width of the initial hard transient phase of the March 5 event; (iv) confine the energy that was radiated in the soft tail of that burst; (v) reduce the Compton scattering cross-section sufficiently to generate a radiative flux that is $\sim 10^4$ times the (non-magnetic) Eddington flux; (vi) decay significantly in $\sim 10^4$ - 10^5 yr, as is required to explain the activity of soft gamma repeater sources on this time-scale; and (vii) power the quiescent X-ray emission $L_X \sim 7 \times 10^{35}$ erg s $^{-1}$ observed by Einstein and ROSAT as it diffuses the stellar interior. We propose that the 1979 March 5 event was triggered by a large-scale reconnection/interchange instability of the stellar magnetic field, and the soft repeat bursts by cracking of the crust.

The epoch folded pulse profile of SGR 1900 + 14 (2-20 keV) for the May 1998 RXTE observations (Kouveliotou et al., 1999).

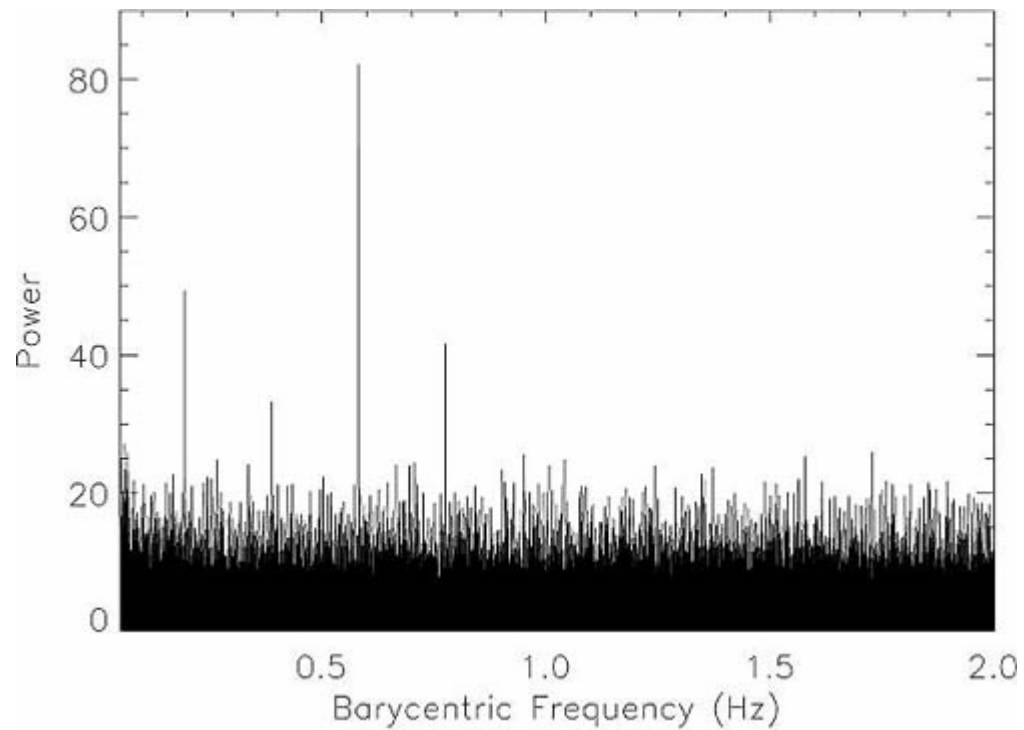


The epoch folded pulse profile of SGR 1900 + 14 (2-20 keV) for the August 28, 1998 RXTE observation. The plot is exhibiting two phase cycles (Kouveliotou et al., 1999).

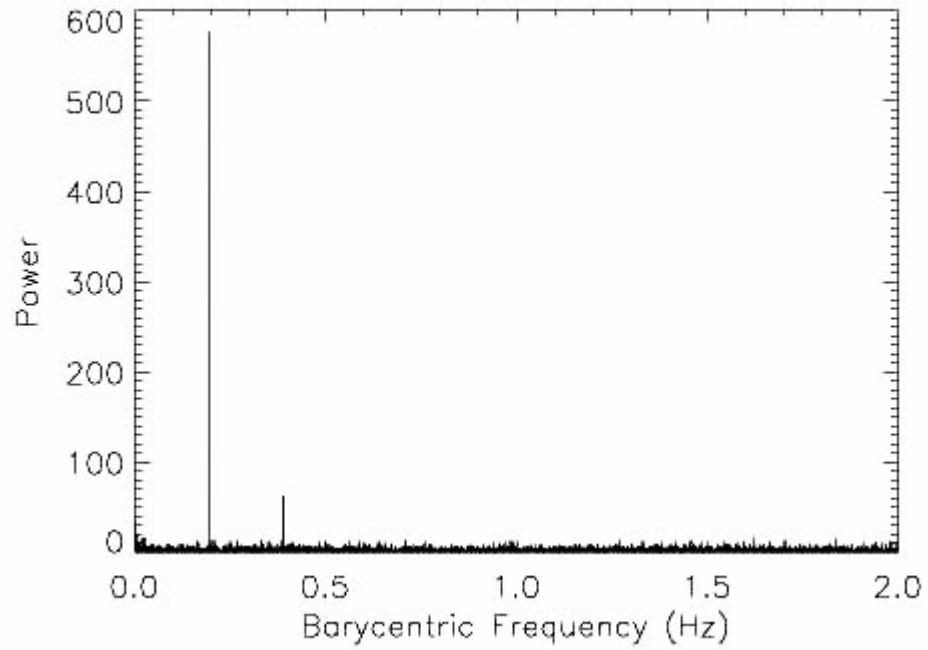


Pulse shape is changing, making errors in finding derivative of the period.

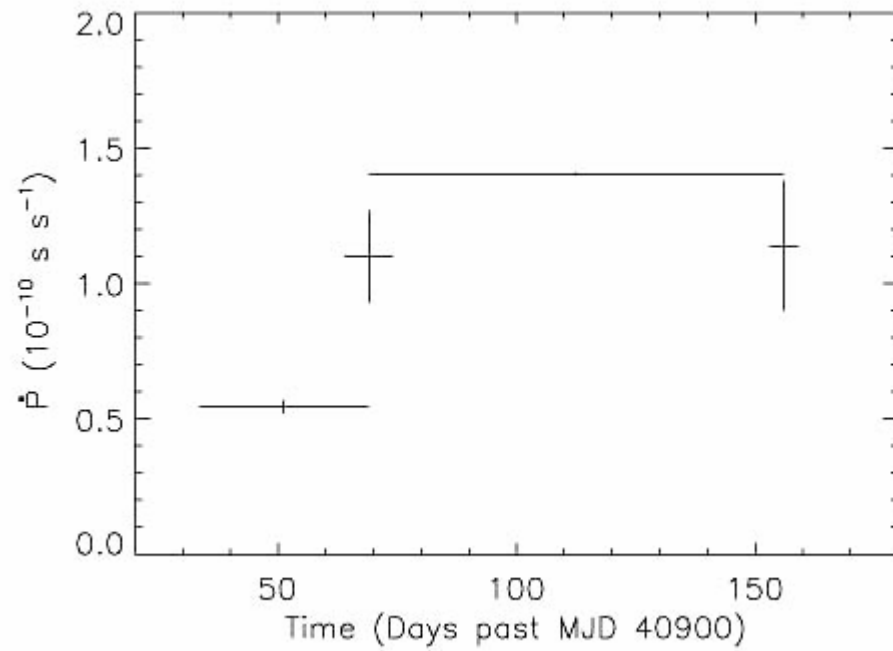
The Power Density Spectrum of the May 1998 RXTE observations of SGR 1900 + 14 . The highest peak in the spectrum corresponds to the fundamental period of 5.159142 s; the three less intense peaks are the harmonics (Kouveliotou et al., 1999)



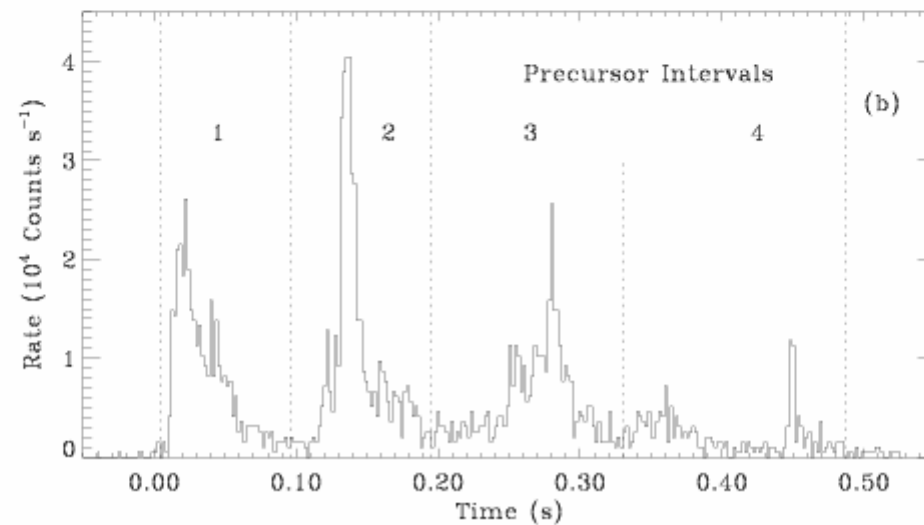
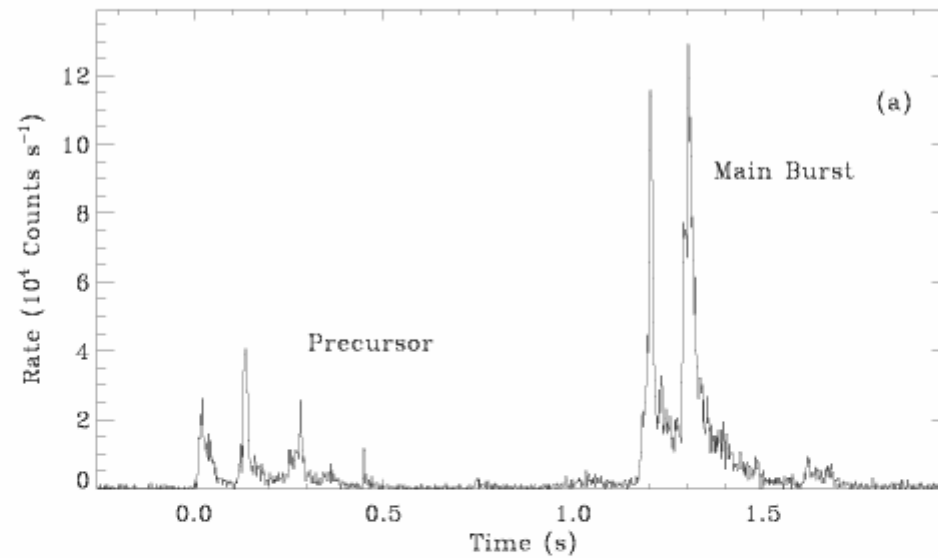
PDS of the August 28, 1998 RXTE observation. The two highest peaks are the fundamental period at 5.160199 s, and its second harmonic (Kouveliotou et al., 1999).



The evolution of "Period derivative" versus time since the first period measurement of SGR 1900+14 with ASCA. The time is given in Modified Julian Days (MJDs) (Kouveliotou et al., 1999)

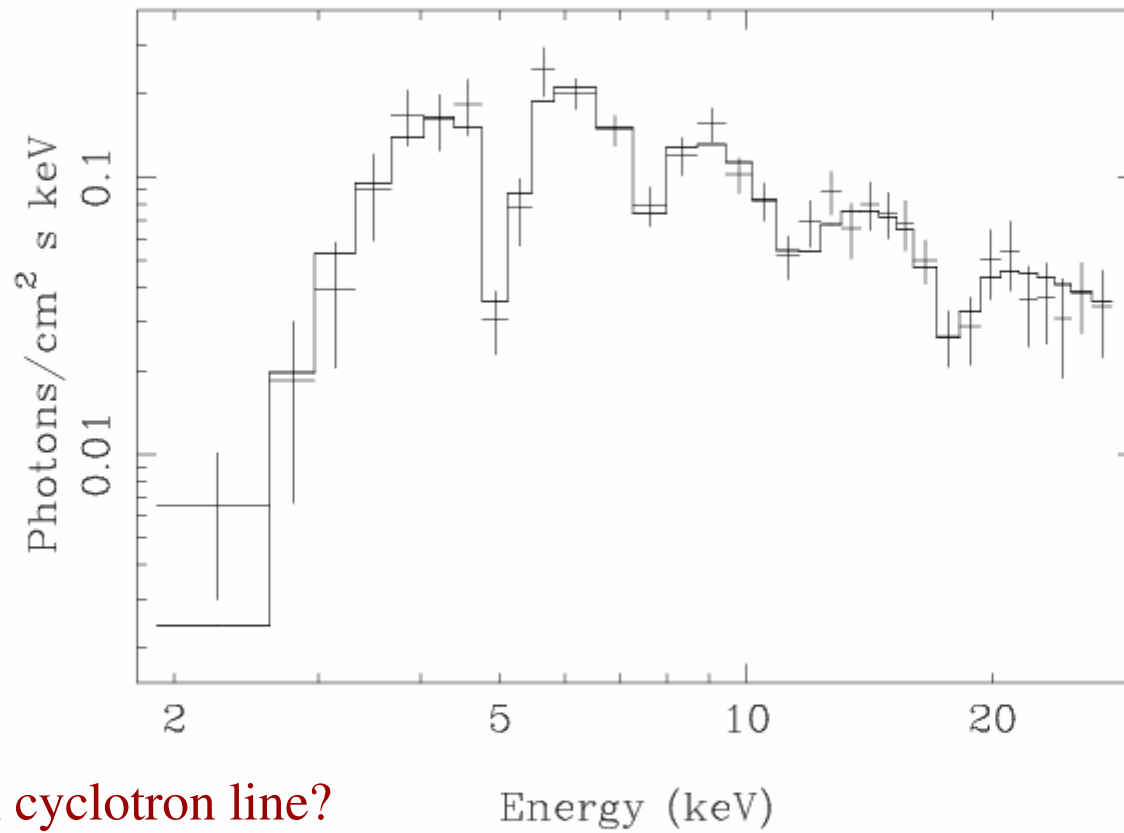


The history of the outburst from SRG 1806-20 (RXTE/PCA 2-60 keV). The top panel (a) shows a bright burst preceded by a long, complex precursor. The bottom panel (b) shows the precursor intervals used in the spectral analysis (Ibrahim et al., 2002).



SGR 1806-20:

spectrum and best-fit
continuum model for the
second precursor interval
with 4 absorption lines
(RXTE/PCA 2-30 keV),
Ibrahim et al. (2002)



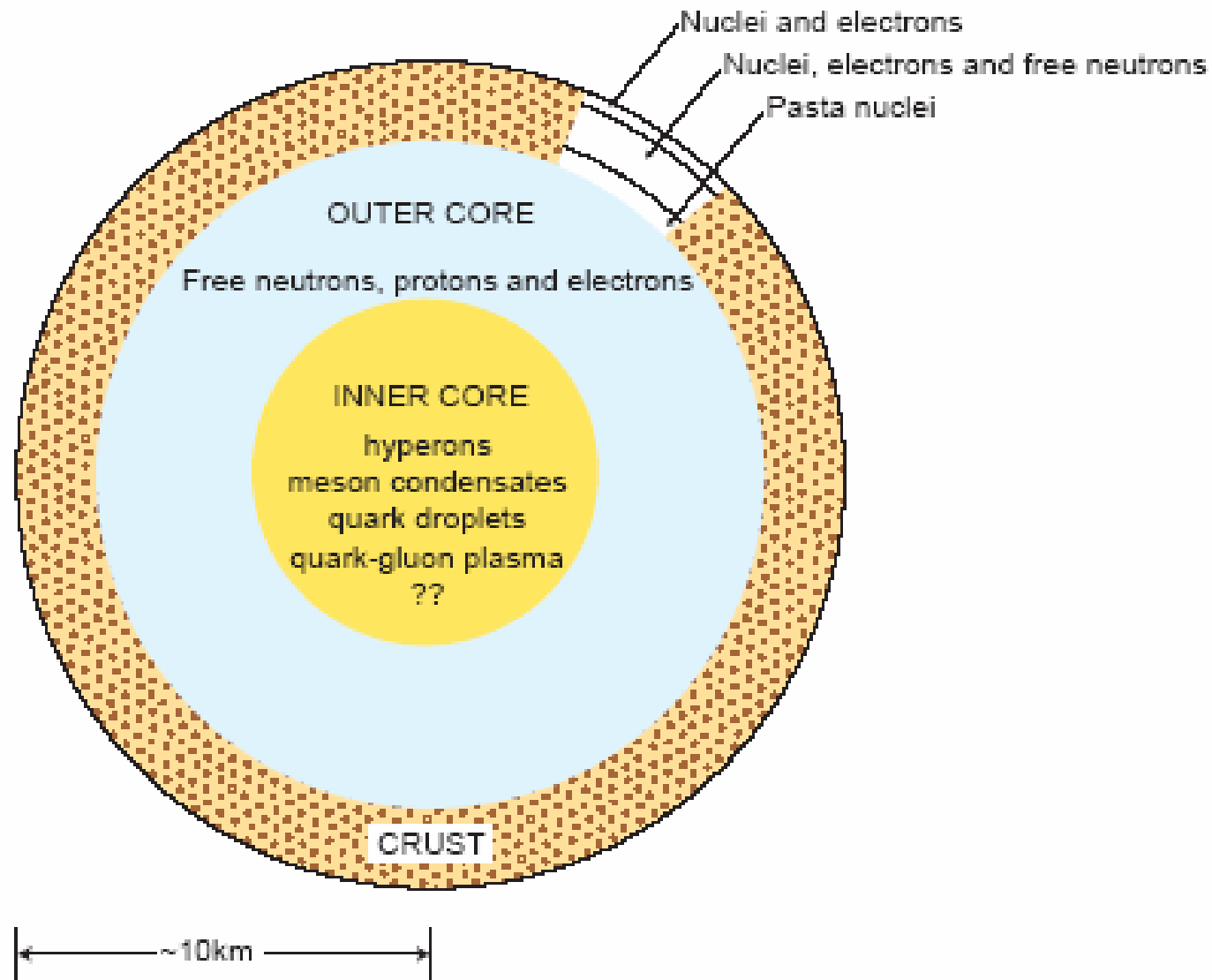
Proton or electron cyclotron line?

**Rotation energy losses are much less than observed (magnetic ?), so
B estimations using dP/dt are not justified.**

**Giant bursts in nearby galaxies (short GRB) – 2 recently have been found
(statistically should be see about 10 short GRB)**

Jumps in dP/dt , in pulse form -- not seen in other pulsars

Cyclotron lines: proton radiation (?)



Schematic cross section of a neutron star.

Cooling of hot dense matter (new born neutron star)

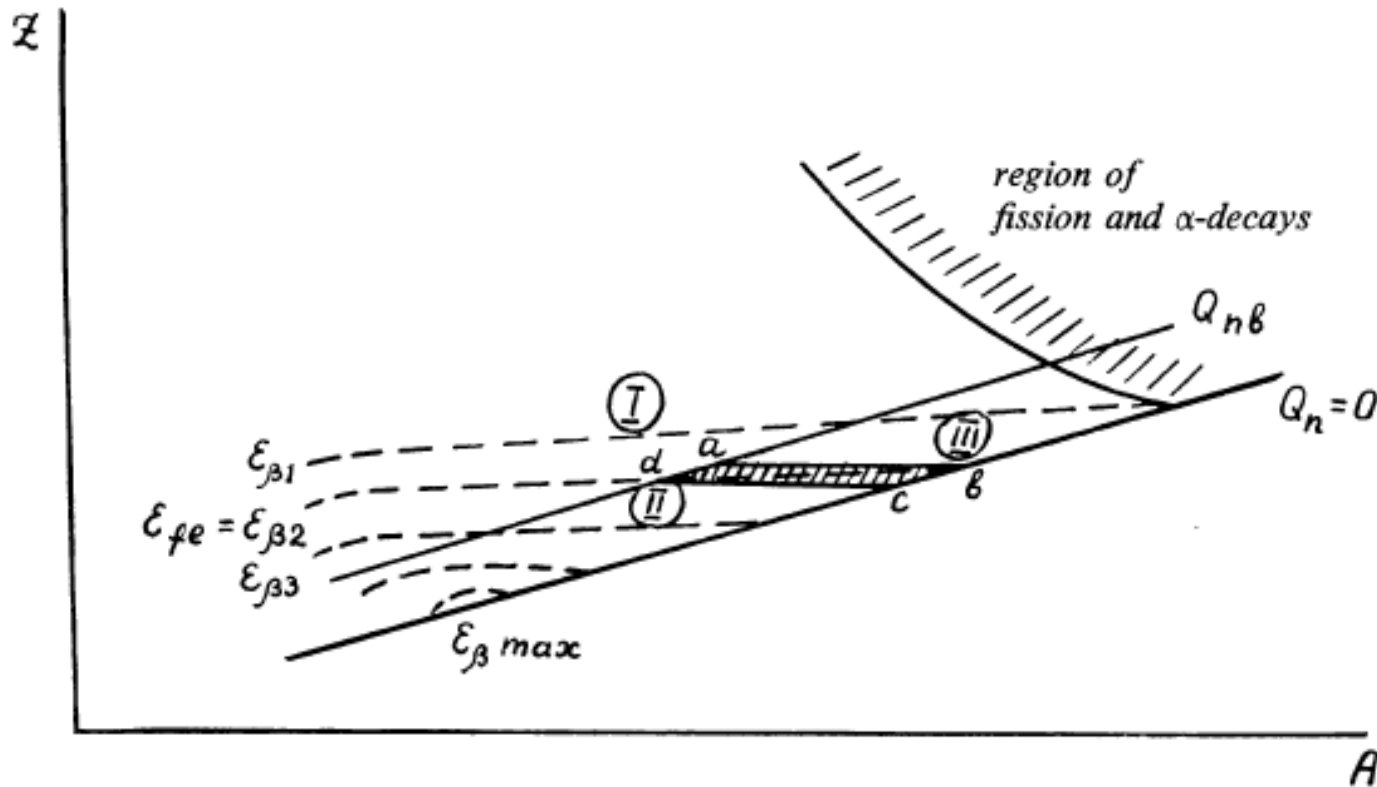


Fig. 4. The formation of chemical composition at the stage of limiting equilibrium. The thick line $Q_n = 0$ defines the boundary of the region of existence of nuclei, the line Q_{nb} separates region I, where photodisintegration of neutrons is impossible from regions II and III. The dashed lines indicate a level of constant $\varepsilon_\beta = Q_p - Q_n$; $\varepsilon_{\beta 1} < \varepsilon_{\beta 2} < \dots < \varepsilon_{\beta \max}$. In region I - $Q_n > Q_{nb}$; in region II - $Q_n < Q_{nb}$, $\varepsilon_{fe} < \varepsilon_\beta$; and in region III - $Q_n < Q_{nb}$, $\varepsilon_{fe} > \varepsilon_\beta$. The line with the attached shading indicates a region of fission and α -decay. The shaded region $abcd$ determines the boundaries for the values of (A, Z) with a limited equilibrium situation, at given values of $Q_{nb}(T)$ and $\varepsilon_{fe}(\rho)$.

G. S. BISNOVATYI-KOGAN and V. M. CHECHETKIN

Astrophysics and Space Science 26 (1974) 25-46.

Nonequilibrium layer of maximal mass

$$M_{od} = \frac{4\pi R^4}{GM} (P_2 - P_1) \simeq 0.1 (P_2 - P_1) = 2 \cdot 10^{29} \text{ g} = 10^{-4} M_{\text{Sun}}$$

$$\rho_1 \simeq \mu_e 10^6 \left(\frac{8}{0.511} \right)^3 \simeq 3.8 \times 10^9 \mu_e \text{ gm cm}^{-3}.$$

$$\rho_2 \simeq \mu_e 10^6 \left(\frac{33}{0.511} \right)^3 \simeq 2.7 \times 10^{11} \mu_e \text{ gm cm}^{-3}$$

$$E_n \approx 4 \times 10^{17} (P_2 - P_1) \text{ эрг} \approx 10^{48} \text{ эрг}$$

$$P_1 = 7.1 \times 10^{27} \text{ in cgs units,}$$

$$P_2 = 2.1 \times 10^{30} \text{ in cgs units.}$$

**PULSED GAMMA-RAY EMISSION FROM NEUTRON
AND COLLAPSING STARS AND SUPERNOVAE***

G. S. BISNOVATYI-KOGAN, V. S. IMSHENNIK, D. K. NADYOZHIN,
and V. M. CHECHETKIN

and the spectrum of emission. In case (3) ejection of chemically non-equilibrium matter from the neutron star leads to an intensive emission which is produced due to fission of superheavy nuclei, β -decay of radioactive elements and radiative capture of free neutrons. Ejection of matter from the neutron stars may be related to the observed jumps of periods of pulsars. From the observed gain of kinetic energy of the filaments of the Crab Nebula ($\sim 2 \times 10^{41}$ erg) the mass of the ejected material may be estimated ($\sim 10^{21}$ g). This leads to energies of the γ -ray bursts of the order of 10^{38} – 10^{39} erg, which agrees fully with observations at the mean distance up to the sources 0.25 kpc. As distinct from the outbursts of supernovae it would seem that no difficulties concerning the burst frequency and the spectrum of emission are encountered. From the mechanisms of γ -ray emission examined here the

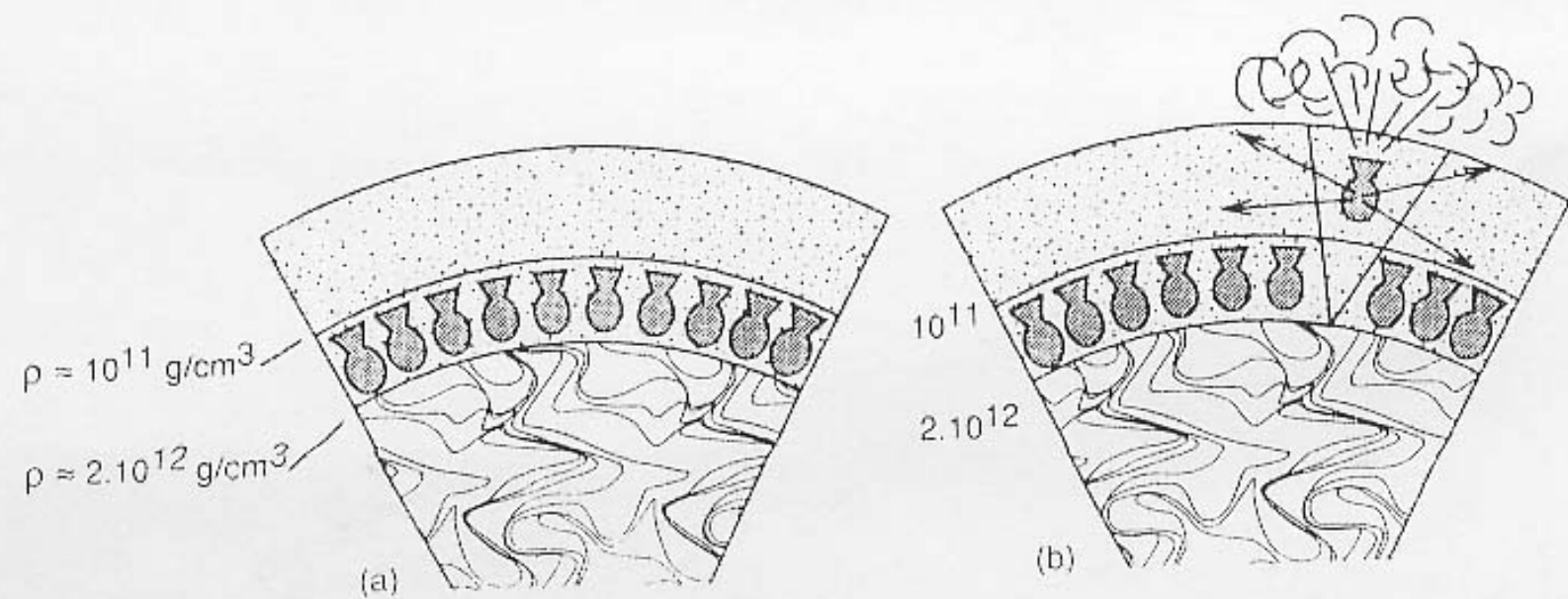
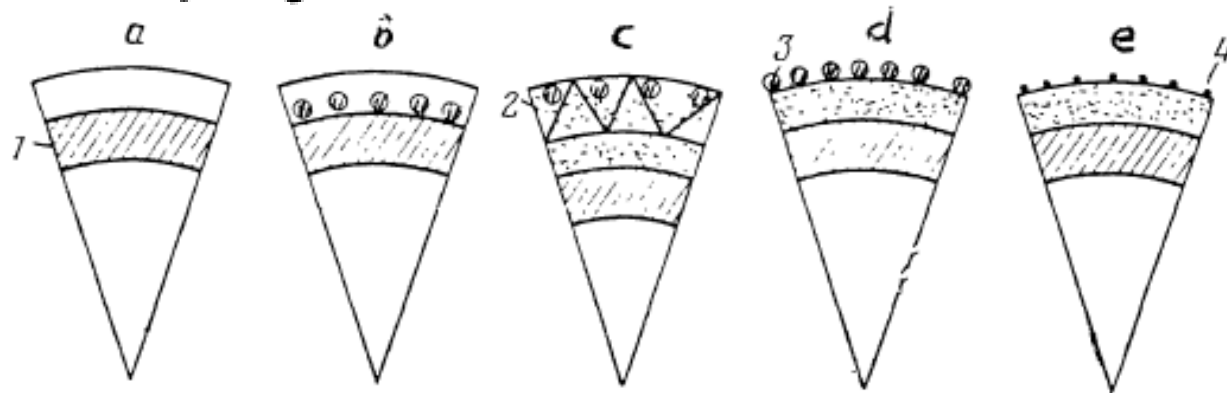


Fig. 1—The schematic picture of nonequilibrium layer in the neutron star: a) in quiescent stage; b) after starquake and nuclear explosion.

Gamma-ray bursts as a manifestation of the inherent activity of neutron stars

G. S. Bisnovaty-Kogan and V. M. Chechetkin



F Fig. 5. Schematic picture of gamma-ray burst formation 5 March 1979; a - envelope in static equilibrium, 1 - nonequilibrium layer; b - after starquake, c - after nuclear explosion, 2 - shock wave, d - expansion of the cloud (3) and explosions there, e - pulsar stage, 4 - hot corona

A numerical model of an explosion near the surface of a neutron star and gamma-ray bursts

G. S. Bisnovatyi-Kogan, S. I. Blinnikov, and A. F. Zakharov

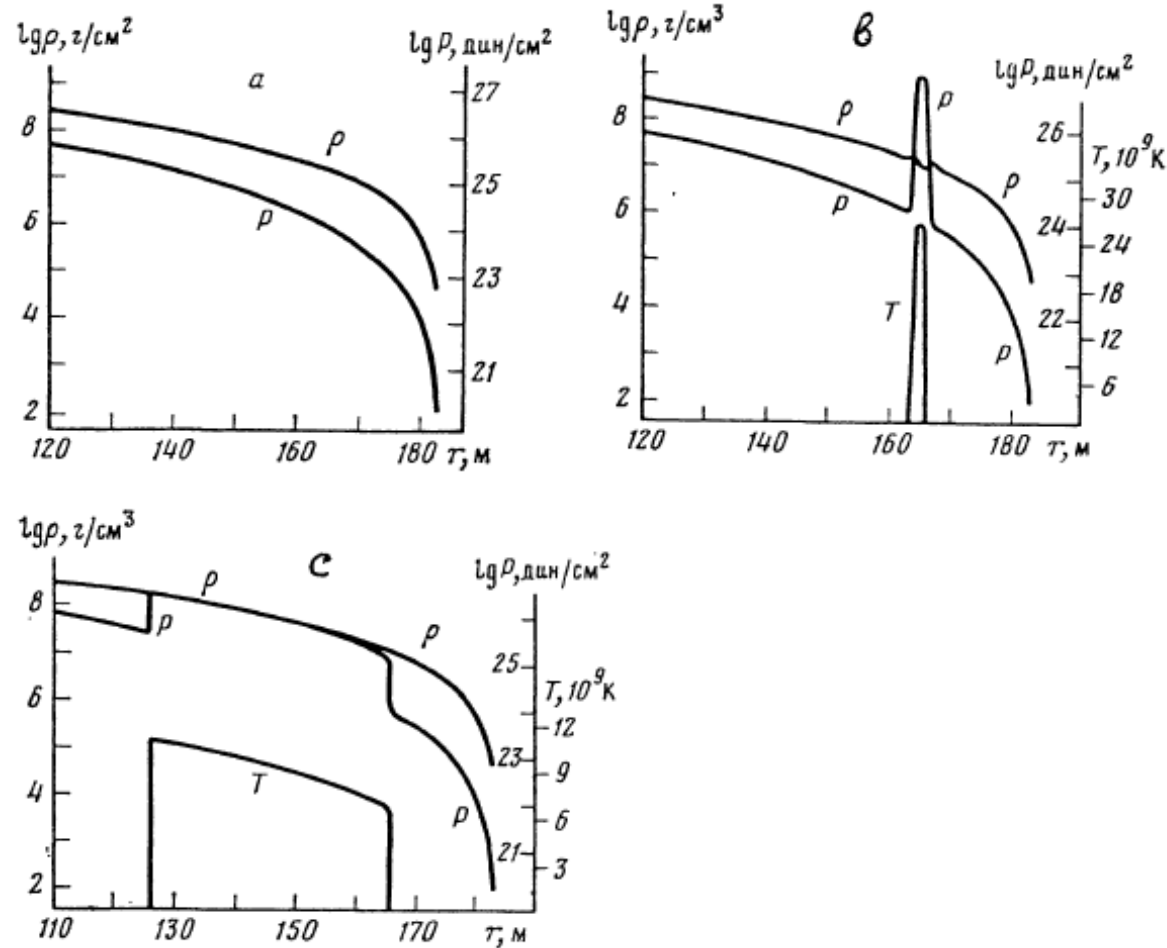


Fig. 3. Density, pressure and temperature distributions in the envelope of the neutron star with $M=1M_{\odot}$.

Progress of Theoretical Physics
Vol. 62 No. 4 pp. 957-968 (1979)

Nuclear Compositions in the Inner Crust of Neutron Stars

Katsuhiko Sato

Department of Physics, Kyoto University, Kyoto 606

(Received February 26, 1979)

It is likely that matter in a neutron star crust is compressed by accreting matter and/or by the slowingdown of its rotation after the freezing of thermonuclear equilibrium. The change of nuclear compositions, which takes place during the compression, has been investigated.

If the initial species of nuclei is ^{56}Fe , the charge and the mass number of nuclei decrease as a result of repeated electron captures and successive neutron emissions in the initial stage of compression. The nuclear charge and mass are then doubled by pycnonuclear reactions. The final values of the charge numbers of the nuclei in the inner crust at densities $\rho < 10^{13.7}\text{g/cm}^3$ are less than 25, which are about one third of those for the conventional cold catalyzed matter. This result reduces the shear modulus of the crust to one half of the conventional value which makes the magnitude of star quakes weaker.

A Gvozdev, I.Ognev (Yaroslavl university)
are constructing model of a giant
SGR bursts with huge energy
production, basing on the idea of nuclear explosion.

**Collimation in Giant SGR bursts may decrease the
energy output several orders of magnitude**

Conclusions

- 1. GRB – cosmological objects of unknown nature
(BH+heavy magnetized disk ?)**
 - 2. SGR – highly active, slowly rotating neutron stars**
 - 3. Most popular SGR interpretation, as magnetars**
 - 4. Nonequilibrium layer is formed in the neutron star crust, during NS cooling, or during accretion onto it .**
- It may be important for NS cooling, glitches, and explosions, may be connected with SGR**

Solar Physics **121**: 187–196, 1989.

**SOLAR AND STELLAR MAGNETIC FIELDS AND
STRUCTURES: OBSERVATIONS**

JEFFREY L. LINSKY

*Joint Institute for Laboratory Astrophysics, National Institute of Standards and Technology, and the
University of Colorado, Boulder, CO 80309–0440, U.S.A.*

“If the Sun did not have a magnetic field, it would be as uninteresting a star as most astronomers believe it to be.”

attributed to ROBERT B. LEIGHTON

“Magnetic fields are to astrophysics what sex is to psychoanalysis.”

HENK VAN DE HULST (1988)